

**The formation and characterization of poly-ion complex generated  
through the interaction between glycosaminoglycans and polyamines**

グリコサミノグリカンとポリアミンから成るポリイオンコンプレックスの  
物性及び体内動態評価

2016 年

葛 丹



千葉大学学位論文

**The formation and characterization of poly-ion complex generated  
through the interaction between glycosaminoglycans and polyamines**

グリコサミノグリカンとポリアミンから成るポリイオンコンプレックスの  
物性及び体内動態評価

2016 年

千葉大学大学院医学薬学府先端創薬科学専攻

病態分析化学研究室

葛 丹



# CONTENTS

Introduction.....	1
Chapter 1 The formation and characterization of poly-ion complex generated through the interaction between chondroitin sulfate and polyamines	
1.1. Introduction.....	5
1.2. Experimental.....	7
1.2.1. Chemicals and Materials.....	7
1.2.2. PIC Formation.....	7
1.2.3. The Effect of pH Value on the PIC Formation Efficiency.....	8
1.2.4. Preparation of Low Molecular Weight Chondroitin Sulfate.....	11
1.2.5. Particle Size and $\zeta$ -Potential Determination.....	12
1.2.6. Surface Structure Analysis.....	13
1.2.7. Absorption of Orally Administered PIC in Mice.....	13
1.2.8. Determination of CS Contents in Mouse Plasma.....	14
1.2.9. Preparation of Unusual Polyamines.....	16
1.3. Results and Discussion.....	17
1.3.1. Preparation of Poly-ion Complex.....	17
1.3.2. Effect of Mixing Concentration Ratio between CS and SPM on PIC Formation Efficiency.....	20
1.3.3. Effect of pH Value on PIC Formation Efficiency.....	22
1.3.4. Effect of the Molecular Size of CS on PIC Formation Efficiency.....	24
1.3.5. Effect of Unusual Polyamines on PIC Formation Efficiency.....	27
1.3.6. Effect of PIC Formation on the Oral Intake of CS in Animal Models.....	30
1.4. Summary.....	34

Chapter 2	The formation and characterization of poly-ion complex generated through the interaction between heparin and polyamines	
2.1.	Introduction.....	35
2.2.	Experimental.....	36
2.2.1.	Chemicals and Materials.....	36
2.2.2.	PIC Formation.....	37
2.2.3.	Effect of Mixing Concentration Ratio between Heparin and Polyamines on PIC Formation Efficiency.....	37
2.2.4.	The $\zeta$ -Potential Determination.....	37
2.2.5.	Effect of PIC Formation on the Oral Intake of Heparin in Mouse Models....	38
2.2.6.	Determination of Heparin Contents in Mouse Plasma.....	38
2.3.	Results and Discussion....	40
2.3.1.	Preparation of Poly-ion Complex....	40
2.3.2.	Effect of Mixing Concentration Ratio between Heparin and Polyamines on PIC Formation Efficiency.....	42
2.3.3.	Effect of PIC Formation on the Oral Absorption of Heparin in Animal Models. ....	43
2.4.	Summary.....	44
	Conclusion.....	46
	Acknowledgements.....	48
	References.....	49
	List of publication.....	55
	Dissertation committee.....	56

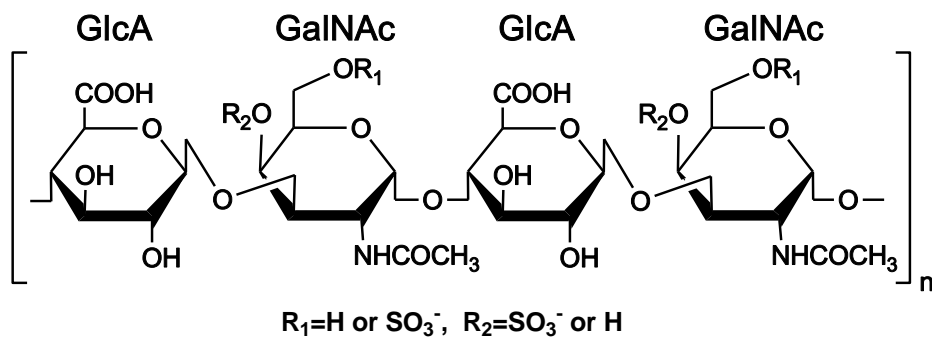
## Introduction

Glycosaminoglycans (GAGs) are long linear polysaccharides constructed by repeating disaccharide units. The repeating unit consists of an hexosamine [*N*-acetylglucosamine (GlcNAc) or *N*-acetylgalactosamine (GalNAc)] along with a uronic acid [glucuronic acid (GlcA) or iduronic acid (IdoA)] or galactose.<sup>1,2)</sup> GAGs ubiquitously exist in the extracellular matrix and cartilaginous tissues with molecular weight ranging from thousands to hundreds of thousands, and are always attached to the serine residue of the core protein to form proteoglycan (PG), playing an important physiological role through the interaction with growth factor or cell adhesion molecules.<sup>3,4)</sup>

Chondroitin sulfate (CS), heparin (HP), heparan sulfate (HS) and hyaluronic acid (HA) have been well known as the representative GAG (Fig. I). Especially, CS consists of the disaccharide repeating units of the structure  $[\rightarrow 4)\text{-}\beta\text{-D-GlcA-(1}\rightarrow 3)\text{-}\beta\text{-D-GalNAc}(\beta 1\rightarrow)]_n$ , which can be substituted with *O*-sulfo groups at various positions. CS has been well studied for its anti-inflammatory function and chondroprotective properties<sup>5-10)</sup> and as the major component of articular cartilage, nowadays CS has been developed as the commercial drug or dietary supplement for the treatment or improvement of arthritic diseases such as osteoarthritis (OA). However, because CS always bears highly negative surface charge and possesses high molecular weight (5 ~ 50 kDa),<sup>11-14)</sup> it is difficult for CS to be effectively absorbed through the gastrointestinal tract. On the other hand, heparin consists of a variably sulfated repeating disaccharide unit that comprises glucuronic acid or iduronic acid along with glucosamine. Heparin is a heterogeneous poly-dispersed mixture of polysaccharides ranging from 3 ~ 30 kDa in molecular weight with an average molecular mass of 15 kDa.<sup>15-17)</sup> Heparin is widely used as an anticoagulant in the clinical researches and has antithrombotic efficacy.<sup>18-20)</sup> Whereas, similarly to CS, the oral absorption efficiency of heparin is undesirable as well owing to its large

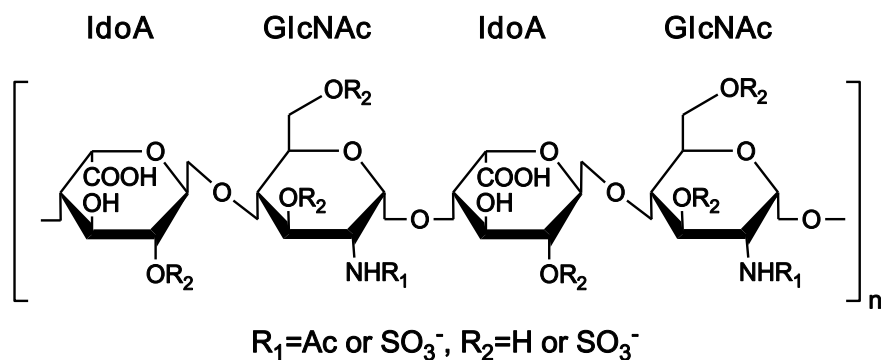
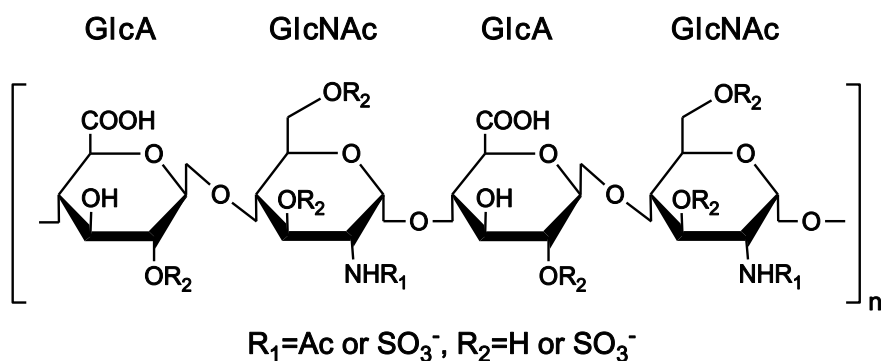
molecular size and highly negative surface charge density. Therefore, heparin can only be injected intravenously or subcutaneously, which limits its application.

(a)



**Chondroitin Sulfate (Mw. 5 ~ 50 kDa)**

(b)



**Heparin (Mw. 3 ~ 30 kDa)**

**Fig. I Structures of glycosaminoglycans.**



Polyamines (putrescine: PUT, spermidine: SPD and spermine: SPM) (Fig. II), ubiquitously distributed in natural products at high concentrations, are organic molecules having two or more primary amino,  $-NH_2$  groups.<sup>21,22)</sup> Intracellular polyamines exist as polyamine-RNA complexes, despite their binding affinity for other acidic molecules, such as DNA, phospholipids and ATP. Selective structural changes of specific RNA structures by polyamines have been suggested to play an important role in cellular proliferation and differentiation.<sup>21,23)</sup>

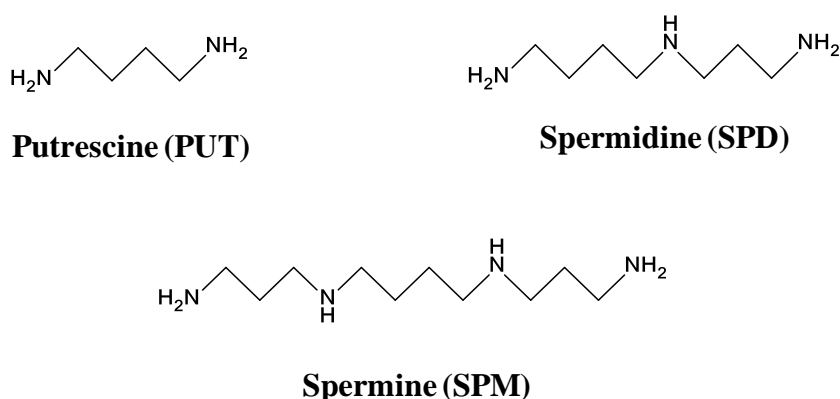


**Fig. II Structures of polyamines.**

Polyamines bound to nucleic acids can induce aggregation, structural changes of DNA and can stabilize DNA *in vitro*.<sup>24-28)</sup> Based on these insights, SPM and polyamine analogs such as poly (L-lysine), polyethylenimine, *etc.*, have been examined for the construction of nanoparticles containing siRNA or plasmid DNA for delivering genes to specific target organs or cultured cells.<sup>29-34)</sup> Interestingly, poly-ion complex (PIC) formation through the electrostatic interaction between polylysine and CS, has been reported.<sup>35)</sup> This report inspired us to attempt to prepare PICs by mixing glycosaminoglycans and natural polyamines in aqueous solutions and investigate their effect on GAG oral absorption. Since polyamines are found at high concentrations in natural foods, they are considered to have extremely low toxicity.

In the present study, the efficient formation of PICs from GAGs and polyamines has been accomplished. The dependence on the mixing ratio between GAGs and

polyamines, molecular weight of GAGs, nature of polyamines, and the pH for PIC formation have been investigated. The preparation of PICs, simultaneously possessing high formation efficiency and nearly neutral surface charges, that were considered to be important factors for the oral absorption of CS, was established from 15 kDa of CS and SPM. These results suggest that PIC generated by the interaction of CS and polyamines might represent a promising core structure for the development of CS delivery system in gastrointestinal tract. In addition, studies are underway for investigating the efficacy of PIC generated from heparin.

# Chapter 1

## The formation and characterization of poly-ion complex generated through the interaction between chondroitin sulfate and polyamines

### 1.1. Introduction

Chondroitin sulfate (CS), a sulfated linear glycosaminoglycan (GAG), is constructed by disaccharide repeating units of the structure  $[\rightarrow 4)\text{-}\beta\text{-D-GlcA-}(1\rightarrow 3)\text{-}\beta\text{-D-GalNAc}(\beta 1\rightarrow)]_n$ , where GlcA represents glucuronic acid and GalNAc means *N*-acetylgalactosamine,<sup>36)</sup> which can be substituted with *O*-sulfo groups at various positions (Fig. 1-1). CS contains, on average, one sulfo group per disaccharide repeating unit at either C-4 or C-6 position of GalNAc. The “A-type unit,” defined as  $[\rightarrow 4)\text{-}\beta\text{-D-GlcA-}(1\rightarrow 3)\text{-}\beta\text{-D-GalNAc4S}(\beta 1\rightarrow)]$  (where “S” designates a sulfo group) is a predominant disaccharide in mammalian or chicken tracheal cartilage CS, while the “C-type unit,” defined as  $[\rightarrow 4)\text{-}\beta\text{-D-GlcA-}(1\rightarrow 3)\text{-}\beta\text{-D-GalNAc6S}(\beta 1\rightarrow)]$ , is a major disaccharide found in shark or salmon nasal cartilage CS.<sup>37,38)</sup> CS is widely distributed in animal tissues and may play an important role in different types of metabolic reactions as well as a protective agent of the joints, the internal walls of blood vessels, skin, bones, *etc.*

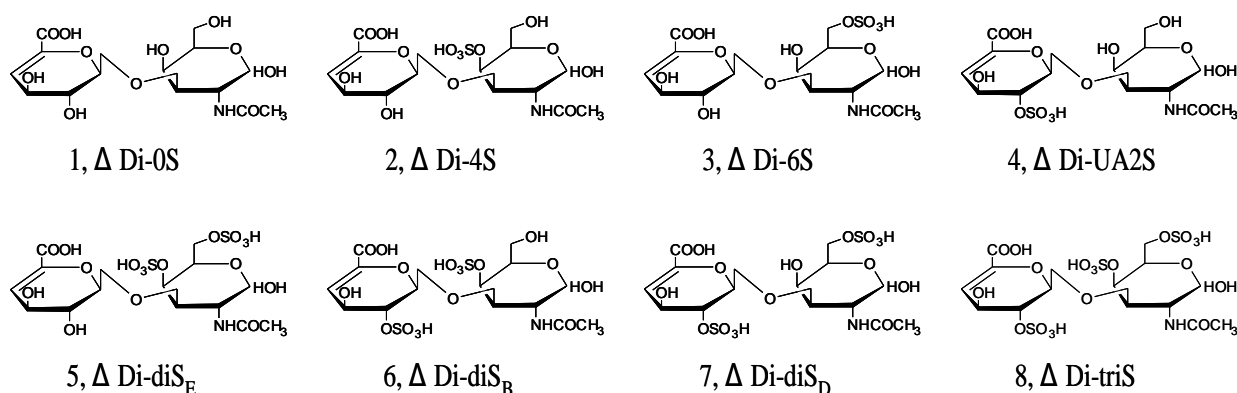


Fig. 1-1 Structures of unsaturated chondro-disaccharides.

Since CS stabilizes fibrous and cellular elements of the connective tissue and at the same time lubricates and protects the membranes in joints,<sup>39-42)</sup> CS has become increasingly popular as an ingredient in health foods for the symptomatic treatment of joint diseases, such as joint rheumatism and osteoarthritis. However, CS is poorly absorbed through the gastrointestinal tract on account of its high molecular weight (5 ~ 50 kDa) and highly negative surface charge.<sup>11-14)</sup> Therefore, development of CS absorption system through the intestinal barrier is one of the critical challenges for the successful application of CS in the treatment of osteoarthritis.

There have been several reports demonstrating that the preparation of self-assembling micelles as the CS drug carrier system was developed based on the conjugation with  $\alpha$ -linoleic acid.<sup>43)</sup> In addition, novel nanomaterials are being developed to improve the oral bioavailability of low molecular mass compounds, proteins, and recombinant DNAs.<sup>44)</sup> Thus, there is the possibility that some nanomaterial or macromaterial may be useful for the development of less expensive and safer delivery systems for oral intake of CS.

Under the inspiration of poly-ion complex (PIC), we attempt to mix CS and natural polyamines in aqueous solutions and investigate how the product effects on CS oral absorption. In the current study, we have successfully generated PIC with high formation efficiency utilizing CS and polyamines. Furthermore, the dependence on the mixing ratio between CS and polyamines, molecular weight of CS, nature of polyamines, and the pH for PIC formation have been investigated. The combination of 15 kDa CS and SPM has accomplished the preparation of PIC simultaneously possessing high formation efficiency and nearly neutral surface charges, and has been demonstrated to significantly facilitate the oral absorption efficiency of CS. These results indicate that PIC generated by the interaction between CS and polyamines might represent a promising core structure for the improvement of CS bioavailability in the digestive system.

## **1.2. Experimental**

### **1.2.1. Chemicals and Materials**

Chondroitin sulfate-A (average molecular weight: 15 kDa, 14.0% of  $\Delta$ Di-0S, 49.8% of  $\Delta$ Di-4S, 36.1% of  $\Delta$ Di-6S) from bovine tracheal cartilage was purchased from Shin-Nippon Yakugyo Co., Ltd. (Tokyo, Japan). Chondroitin sulfate-C (Mw. avg 46 kDa, 1.77% of  $\Delta$ Di-0S, 13.7% of  $\Delta$ Di-4S, 70.8% of  $\Delta$ Di-6S, 2.89% of  $\Delta$ Di-diSE, 10.8% of  $\Delta$ Di-diSD) from shark cartilage, chondroitinase ABC (Proteus vulgaris EC 4.2.2.4), the unsaturated disaccharides ( $\Delta$ Di-0S,  $\Delta$ Di-4S,  $\Delta$ Di-6S,  $\Delta$ Di-diSE,  $\Delta$ Di-diSB,  $\Delta$ Di-diSD, and  $\Delta$ Di-triS) were purchased from Seikagaku Corp. (Tokyo, Japan). Fractioned CS standard samples (Mw. 6 kDa, 13 kDa, 31 kDa; 44 kDa) for molecular weight determination were prepared as described previously in literature.<sup>45)</sup> Spermine tetrahydrochloride (SPM·4HCl) was obtained from Nacalai Tesque Inc. (Kyoto, Japan). Tetrabutylammonium hydrogen sulfate (TBA) and titanium dioxide (anatase type, average particle size, 50  $\mu$ m) were obtained from Wako Pure Chemical Co. (Osaka, Japan). 2-cyanoacetamide and deuterium oxide (D<sub>2</sub>O, 99.96 atom% D) were obtained from Sigma-Aldrich Co. LLC. (St Louis, MO, USA). Water used in studies was purified using Q-GARD<sup>®</sup> 1, Millipore. All other chemicals were of analytical reagent grade and used without further purification.

### **1.2.2. PIC Formation**

CS and polyamines were separately dissolved in double-distilled water, with a doubled concentration of the target PIC, and then equivalent volumes of CS solution and polyamine solution were fully mixed with one another to generate PIC. PIC formation efficiency was evaluated by turbidimetric measurement, namely the determination of % transmittance (*T*), using thermo scientific SPECTONIC 20D+ digital spectrophotometer.

### **1.2.3. The Effect of pH Value on the PIC Formation Efficiency**

A 100  $\mu\text{L}$  aliquot of 50 mM SPM aqueous solution was fully mixed with the equal volume of 40 mg/mL of CS, and then the solutions containing PIC were separately adjusted to pH value 1~9 using 1 M HCl or 1 M NaOH. PIC fraction, obtained by the centrifugation at 6,000  $g$  for 5 min, was suspended and precipitated twice, using 1 mL of pH conditioned  $\text{H}_2\text{O}$  to remove the free SPM and CS that did not form PIC. Since PIC formation was unstable under basic conditions (pH value above 9), 400  $\mu\text{L}$  aliquot of 0.2 M NaOH was added to the PIC pellets to dissociate CS and SPM from each other. Free SPM was separated from CS using Amicon<sup>®</sup> Ultra 10 K spin columns by centrifugation at 6,000  $g$  for 30 min at 4°C, and then the separated CS and SPM samples were quantitatively analyzed by high-performance liquid chromatography (HPLC) (Fig. 1-2).

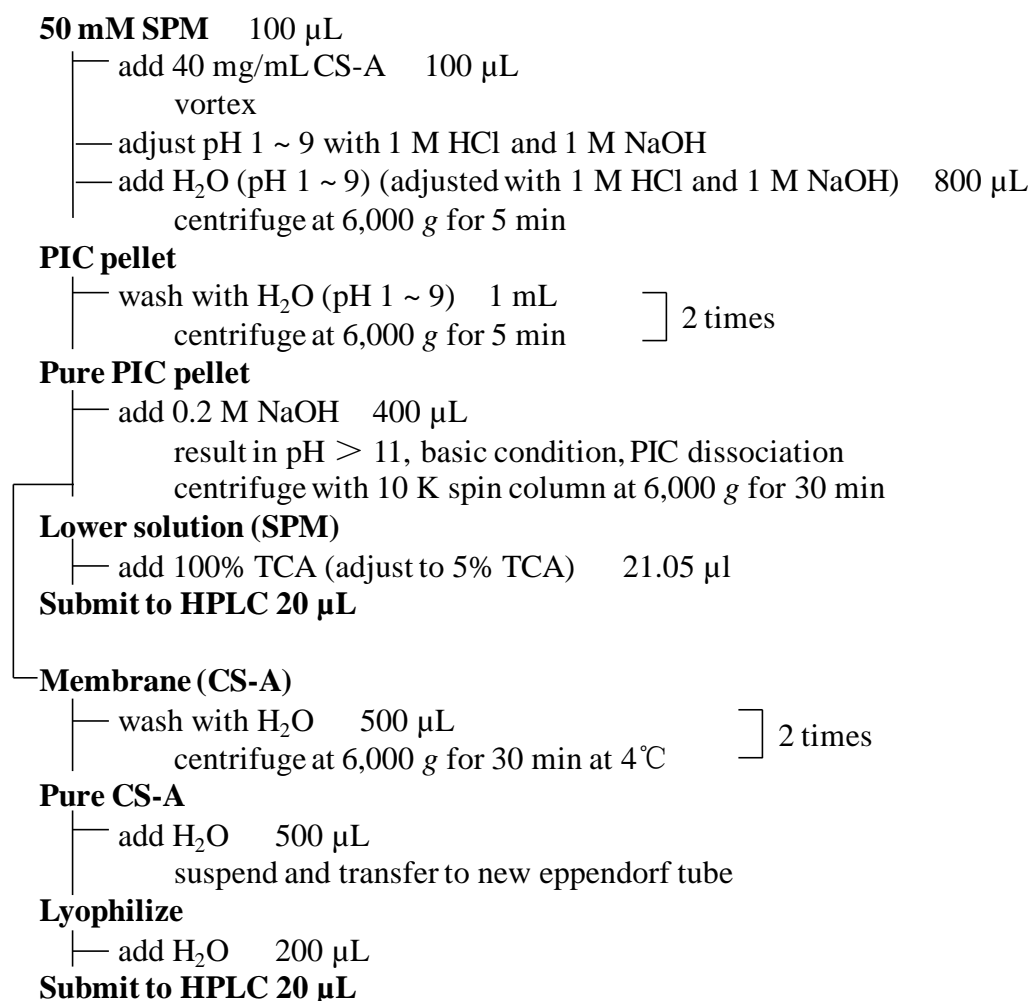


**Fig. 1-2 Isolation of CS and SPM from PIC.**

### **HPLC Conditions**

The HPLC system for CS quantitative analysis comprised two DP-8020 Pumps (Tosoh Corporation, Tokyo, Japan) as the gradient eluent pumps and an NP-FX (II) -1 MINICHEMI Pump (Nihon Seimitsu Kagaku Co. Ltd, Tokyo, Japan) as the post-column reaction solution pump. An AS-8020 (Tosoh Corporation, Tokyo, Japan) Auto Sampler, a CO631A (GL Sciences Inc., Tokyo, Japan) Column Oven, a DB-5 (Shimamura Instrument Co., Tokyo, Japan) Dry Reaction Bath, an FP-1520S (Jasco Corporation, Tokyo, Japan) Intelligent Fluorescence Detector and a DGU-12A (Shimadzu Corporation, Kyoto, Japan) Degasser were also applied to this HPLC

analysis system. Here, an Asahipak NH2P-50 4E column (4.6 mm i.d.  $\times$  250 mm, 5  $\mu$ m, Showa Denko K.K., Tokyo, Japan) was used along with a guard column Asahipak NH2P-50G 4A (4.6 mm i.d.  $\times$  10 mm, 5  $\mu$ m, Showa Denko K.K., Tokyo, Japan). The mobile phases: (A) 0.1 M sodium carbonate buffer (pH 10.0) containing 0.1 M NaCl and (B) 0.1 M sodium carbonate buffer (pH 10.0) containing 1.0 M NaCl were eluted according to the following gradient program: 0 - 20 min (0 - 100% B), 20 - 25 min (100% B), 25 - 27 min (100 - 0% B), 27 - 35 min (0% B) (for initialization). And the flow rate was constantly maintained at 0.5 mL/min. The post-column reaction reagents (1) and (2) were 50 mM guanidine and 1.0 M NaOH, respectively, and the flow rates were both maintained at 0.25 mL/min. The column was kept at the room temperature and the post-column reaction temperature was set at 120°C. The reaction mixture passed the reaction coil (0.5 mm i.d.  $\times$  10 m), fully heated in the reactor to accelerate the reaction, and then was cooled down in the cooling coil (0.25 mm i.d.  $\times$  5 m). The detection wavelength was set at 425 nm with 320 nm of excitation. 0.05, 0.1, 0.5, 1, 2 and 4  $\mu$ g of CS (Mw. 15 kDa) were used as the standard samples to plot the calibration curve for quantitatively determining CS contents in PIC.

The HPLC system for polyamine quantitative analysis comprised an ELITE LaChrom L-7110 Pump (Hitachi High-Technologies Corporation, Tokyo, Japan) as the eluent pump, an NP-FX (II) -1 MINICHEMI Pump (Nihon Seimitsu Kagaku Co. Ltd, Tokyo, Japan) as the post-column reaction solution pump, an ELITE LaChrom L-7200 (Hitachi High-Technologies Corporation, Tokyo, Japan) Auto Sampler, an ELITE LaChrom L-7300 (Hitachi High-Technologies Corporation, Tokyo, Japan) Column Oven and an FP-1520S (Jasco Corporation, Tokyo, Japan) Intelligent Fluorescence Detector. A TSK gel Polyaminepak column (4.6 mm i.d.  $\times$  50 mm, Tosoh Corporation, Tokyo, Japan) was applied in this study and the mobile phase (containing 0.35 M Sodium-citrate, 2 M NaCl, 20% methanol, 0.1% Brij-35 and 0.01% *N*-capric acid (pH 5.3)) was constantly maintained at 0.42 ml/min. The flow rate of the post-column reaction reagent (containing 0.4 mM Borate-KOH, 0.06%



*o*-phthalaldehyde, 37 mM  $\beta$ -mercaptoethanol and 0.1% Brij-35) was also set at 0.42 ml/min. The column temperature was set at 50°C and the detection wavelength was set at 470 nm with 336 nm of excitation. 5  $\mu$ M of SPM dissolved in 5% TCA was utilized as the standard sample.

#### **1.2.4. Preparation of Low Molecular Weight Chondroitin Sulfate**

Low molecular weight (LMW) CS was prepared by photochemical depolymerization with titanium dioxide (TiO<sub>2</sub>) as described in previous literatures with minor modifications.<sup>46,47)</sup> The photochemical reaction device (Sen Lights Corporation, Osaka, Japan) consisted of a VG1500 reaction tank with 5 inlets, a light source (high pressure mercury lamp HL100 CH-4, 100W), a power source (HB100P-1) and water-cooling jacket JW-1G. The apparatus was connected with a water circulating system to cool the lamp.

Briefly, 1 g of CS-A (Mw. 15 kDa) was dissolved in 100 mL of H<sub>2</sub>O with 100 mg of TiO<sub>2</sub> in the VG1500 reaction tank. After being exposed to the light for specified time, molecular weight of CS was monitored by gel permeation chromatography (GPC)-HPLC to obtain 8 kDa and 5 kDa of LMWCS.<sup>45)</sup> After the reaction, the sample was centrifuged at 1,500 g for 5 min at 20°C and the supernatant was filtered through 0.45  $\mu$ m disposable syringe filter unit (Dismic-13HP; Advantec, Tokyo, Japan) to eliminate all of the TiO<sub>2</sub> particles. Then the product solution was neutralized with NaOH, followed by dialysis against water using Spectra/Por® Dialysis Membrane MWCO: 3,500 and ultimately the obtained solution was lyophilized to prepare the LMWCS powder sample.

#### **HPLC Conditions**

The GPC-HPLC system for molecular weight determination consisted of an L-6000 Pump (Hitachi High-Technologies Corporation, Tokyo, Japan) equipped with a Rheodyne Model-7725 Injector with 20  $\mu$ L Sample Loop (Rheodyne Inc., Cotati,

CA, USA), an SPD-6A UV Spectrophotometric Detector (Shimadzu Corporation, Kyoto, Japan) set at 204 nm, and a D-2500 Chromato Integrator (Hitachi High-Technologies Corporation, Tokyo, Japan). The molecular weight of CS was determined using gel permeation chromatography with Asahipak GF-510 HQ column (7.5 mm i.d.  $\times$  300 mm, 5  $\mu$ m, Showa Denko K.K., Tokyo, Japan). Isocratic elution with 10 mM  $\text{NH}_4\text{HCO}_3$  was used at a flow rate of 0.3 mL/min. The fractionated CS standard samples (average molecular weight 6, 13, 31 and 44 kDa) were applied to construct the calibration curve using the retention time plotted against the antilogarithm of molecular weight. Thereby, the average molecular weight of the photodegraded CS was calculated from this calibration curve.

#### **Structural Analysis of LMWCS by $^1\text{H}$ -NMR Spectroscopy**

The chemical structures of CS (Mw. 15 kDa) and LMWCS (Mw. 5 kDa) were verified using proton nuclear magnetic resonance ( $^1\text{H}$ -NMR) spectroscopy on JNM-ECS400 (Jeol Resonance Inc., Tokyo, Japan). 4 mg of each sample was repeatedly dissolved in 600  $\mu$ l of  $\text{D}_2\text{O}$  and lyophilized for twice. The obtained residue was redissolved in 600  $\mu$ l of  $\text{D}_2\text{O}$  and transferred into a 528-pp-8 NMR sample tube (5.0 mm O.D.  $\times$  25 cm, Wilmad-Lab Glass, Vineland, New Jersey, USA) for determination.

#### **1.2.5. Particle Size and $\zeta$ -Potential Determination**

The mean particle sizes of various kinds of PIC samples were determined by dynamic light scattering (DLS) method on the MICROTRAC 9340 UPA-UT151 (Nikkiso Co., Ltd, Tokyo, Japan) equipped with a semi-conductor laser at the wavelength of 780 nm. The  $\zeta$ -potential determinations were performed for each PIC samples on the ELS-Z1 (Otsuka Electronics Co., Ltd, Osaka, Japan) at the 60 V of voltage. Double-distilled water was used as the dispersant and the measurements were carried out at 25°C. The average of three measurements was taken as the final

characteristic parameter.

### **1.2.6. Surface Structure Analysis**

PIC samples generated from CS and polyamines were characterized by Olympus BX51 upright microscope with Olympus DP-70 color camera (Olympus Optical Co., Ltd, Tokyo, Japan) for the particle morphology. 10  $\mu$ L of aqueous PIC sample was poured on a microscope slide to form a sample film for observation.

### **1.2.7. Absorption of Orally Administered PIC in Mice**

All animal experiments were approved by the Institutional Animal Care and Use Committee of Chiba University and carried out according to the guidelines for Animal Research of Chiba University. The ddY mice (female, weighing 28 - 30 g, Japan SLC, Inc, Shizuoka, Japan) were housed at 25°C and 55% RH. A 12 h dark/light cycle was maintained throughout. Mice had free access to standard pellet diet (MF, Oriental Yeast Co., Ltd, Tokyo, Japan) and tap water, and were fasted overnight before the experiment. The solution containing PIC or CS alone was orally administered to each group (containing 6 - 9 mice) at a single dose of 500 mg CS/kg body weight (*ca.* 15 mg/each animal). Blood samples were collected from the tail vein at time intervals of 0, 0.5, 1, 2, 4, 6, 8, 10 h after oral administration and were anticoagulated with 3.2% trisodium citrate solution at the ratio of blood : 3.2% trisodium citrate = 9 : 1. Each collected sample was immediately centrifuged at 800 g for 15 min to obtain the plasma, which was transferred to a new Eppendorf tube and stored in a deep freezer until used (Fig. 1-3). Additionally, inflammation and wound damage at the digestive system of animals were checked by surgical operation after oral dose of samples.

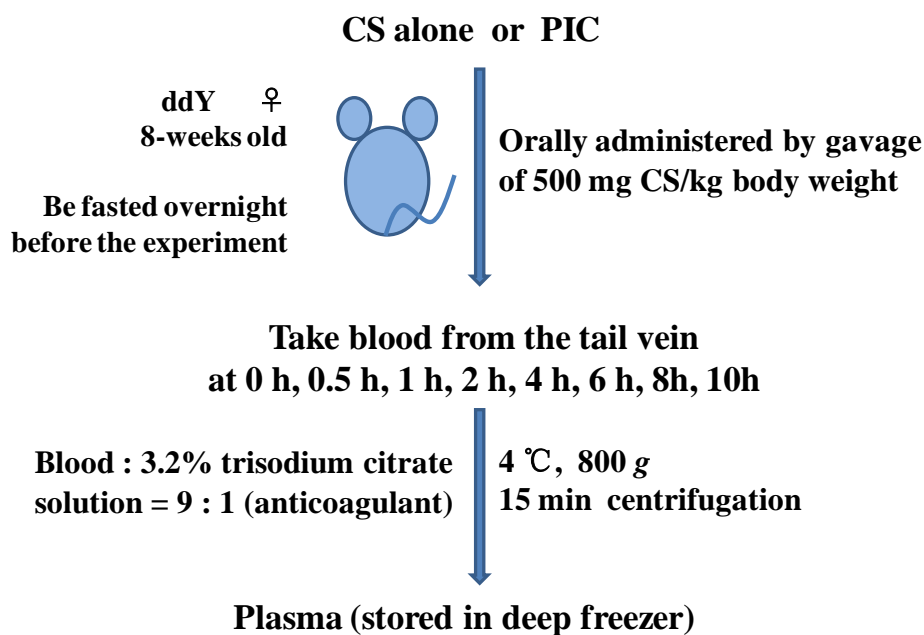


**Fig. 1-3 Schedule of oral administration of PIC in animal models.**

### **1.2.8. Determination of CS Contents in Mouse Plasma**

As shown in Fig. 1-4, mouse plasma (25  $\mu$ L) was treated with 1.3  $\mu$ L of 100% trichloroacetic acid (TCA) (final 5% TCA) and incubated at 4°C for 30 min to obtain free CS. After centrifugation at 20,000 g for 10 min, 15  $\mu$ L of supernatant was neutralized with 1.5  $\mu$ L of 2 M NaOH and diluted with 200  $\mu$ L of H<sub>2</sub>O. The buffer of sample solution was firstly exchanged with 0.2 M tris-acetate (pH 8.0) using Amicon<sup>®</sup> Ultra 3 K spin columns (EMD Millipore Co., MA, USA), followed by buffer exchange with H<sub>2</sub>O. After the collected pure samples were lyophilized, the residues obtained were dissolved in 12.5  $\mu$ L of H<sub>2</sub>O, and then 2.5  $\mu$ L of 0.2 M tris-acetate buffer (pH 8.0) and 2.5  $\mu$ L of 0.1 U/10  $\mu$ L chondroitinase ABC were serially added to each sample. After incubation at 37°C for 18 h, the samples were heated at 100°C for 3 min to inactivate the enzymes and lyophilized again. Finally, the obtained powder samples were redissolved in 60  $\mu$ L of H<sub>2</sub>O and 20  $\mu$ L of each sample was submitted to the unsaturated disaccharide composition analysis HPLC system.

**Plasma 25  $\mu$ L**

- add 100% Trichloroacetic acid (TCA) (adjust to 5% TCA) 1.3  $\mu$ L
- vortex
- stand at 4°C for 30 min
- centrifuge at 20,000 g for 10 min at 4°C

**Supernatant 15  $\mu$ L**

- add 2M NaOH 1.5  $\mu$ L
- add H<sub>2</sub>O 200  $\mu$ L

**Sample on ultra filtration membrane (Amikon Ultra 3K)**

- centrifuge at 12,500 g for 15 min
  - wash with 0.2 M tris-acetate buffer (pH 8.0) 200  $\mu$ L
  - centrifuge at 12,500 g for 15 min
  - turn device upside down in clean tube (vortex)
  - centrifuge at 1,000 g for 10 min
  - add H<sub>2</sub>O 200  $\mu$ L
  - centrifuge at 1,000 g for 10 min
- ] 3 times
- ] 2 times

**Lower solution**

- lyophilize
- add H<sub>2</sub>O 12.5  $\mu$ L
- add 0.2 M Tris-acetate buffer (pH 8.0) 2.5  $\mu$ L
- add 0.1 U/10  $\mu$ L chondroitinase ABC 2.5  $\mu$ L
- incubate at 37°C for 18 h
- heat at 100°C for 3 min
- lyophilize
- add H<sub>2</sub>O 60  $\mu$ L

**Submit to HPLC 20  $\mu$ L**

**Fig. 1-4 Pretreatment of plasma for free CS extraction and procedures for CS disaccharide composition analysis by HPLC.**

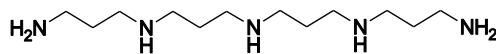
**HPLC Conditions**

The post-column HPLC system for unsaturated disaccharide composition analysis applied the same instruments as CS quantitative analysis. In this study, a DOCOSIL SP100 column (4.6 mm i.d.  $\times$  150 mm, 5  $\mu$ m, Senshu Scientific Co., Ltd, Tokyo, Japan) was used along with a guard column DOCOSIL SP100 (4.6 mm i.d.  $\times$

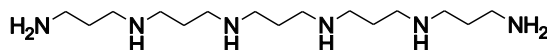
30 mm, 5  $\mu$ m, Senshu Scientific Co., Ltd, Tokyo, Japan). The mobile phases (A) 12% MeOH containing 1.2 mM TBA and (B) 12% MeOH containing 0.2 M NaCl and 1.2 mM TBA were eluted according to the following gradient program: 0 - 10 min (1% B), 10 - 11 min (1 - 10% B), 11 - 30 min (10% B), 30 - 35 min (10 - 60% B), 35 - 40 min (60% B), 40 - 41 min (60 - 1% B), 41 - 50 min (1% B) (for initialization). And the flow rate was constantly maintained at 1.0 ml/min. The post-column reaction reagents (1) and (2) were 0.5% 2-cyanoacetamide and 1.0 M NaOH, respectively. And the flow rates were both maintained at 0.25 ml/min. The column temperature was set at 60°C and the post-column reaction temperature was set at 110°C. The detection wavelength was set at 410 nm with 346 nm of excitation. The mixture containing 4  $\mu$ g/mL of each unsaturated chondro-disaccharide was utilized as the standard sample.

### **1.2.9. Preparation of Unusual Polyamines**

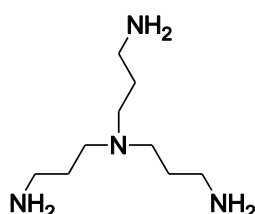
Tris (3-aminopropyl) amine was purchased from Tokyo Chemical Industry Co. (Tokyo, Japan). Tetrakis (3-aminopropyl) ammonium, caldopentamine and caldohexamine were chemically synthesized as reported previously in the literature.<sup>48)</sup> The chemical structures of unusual polyamines were illustrated in Fig. 1-5 and all polyamines used in the study were in the form of their hydrochloride salts. When the unusual polyamine solutions were mixed with 15 kDa of CS to form PICs, the procedures were similar to those described above.



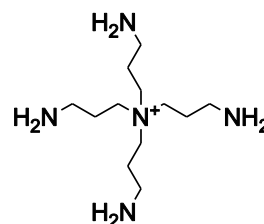
**Caldopentamine (Cdp)**



**Caldohexamine (Cdh)**



**Tris (3-aminopropyl) amine (Mitsubishine)**



**Tetrakis (3-aminopropyl) ammonium (Taa)**

**Fig. 1-5 The chemical structures of unusual polyamines.**

### 1.3. Results and Discussion

#### 1.3.1. Preparation of Poly-ion Complex

At first, we examined whether polyamine spermine (SPM) could aggregate with commercially available CS-A (Mw. 15 kDa) prepared from bovine tracheal cartilage. As shown in Fig. 1-6, the aqueous solution containing CS (40 mg/mL) or SPM (50 mM) was transparent, however, a turbid white solution of PIC was generated when an equivalent volume of CS and SPM solution were fully mixed with one another. Furthermore, after approximately 20 min of settling, the turbid white solution separated into two layers. The upper layer was the aqueous phase, while the lower layer was the PIC phase. But after being thoroughly mixed again using a vortex mixer, the deposited PIC solution could be restored back to a uniform solution.

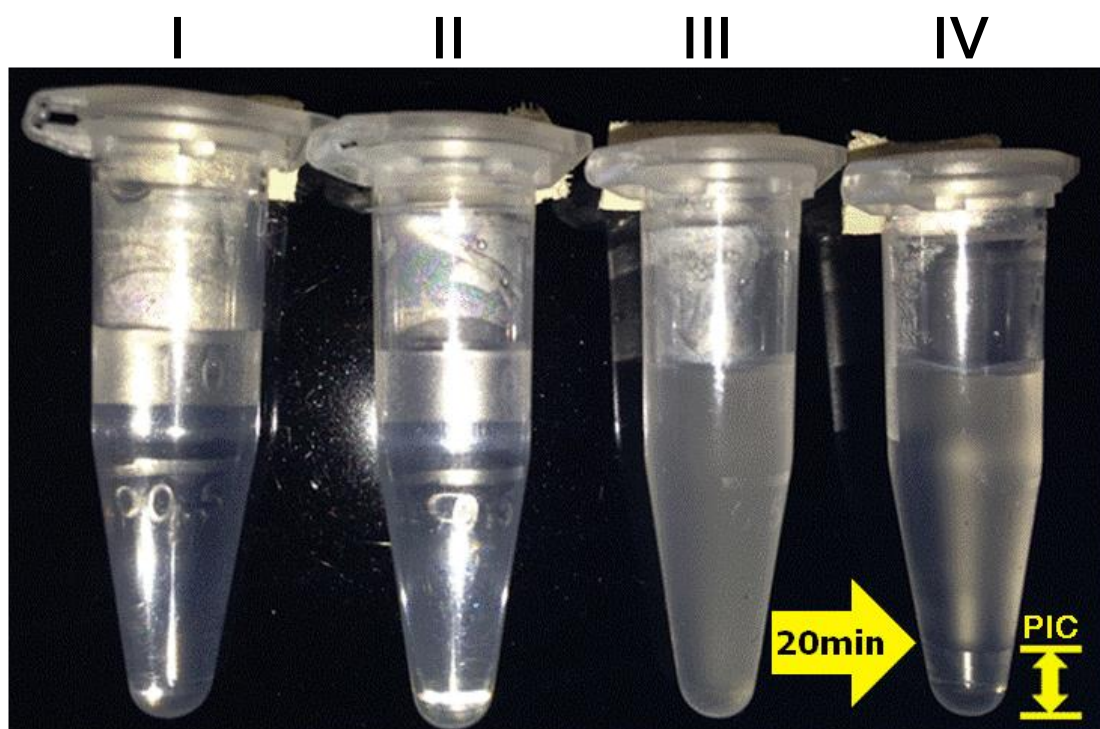


**Fig. 1-6 Photographs of (I) 40 mg/mL of CS, (II) 50 mM of SPM, (III) PIC, (IV) PIC that separated into two layers after standing for about 20 min.**

Morphological characterization of the PIC showed that it was of spherical shape and in a micrometer size range, correlating closely with the particle size ( $3.41 \pm 0.64 \mu\text{m}$ ) measured by dynamic light scattering (Fig. 1-7 and Table 1-1). However, it was observed that adjacent PIC particles quite tended to merge with one another, forming larger particles. Therefore, even though the PIC solution was well mixed, PIC particles with heterogeneously spherical shapes could still be observed under the microscope.



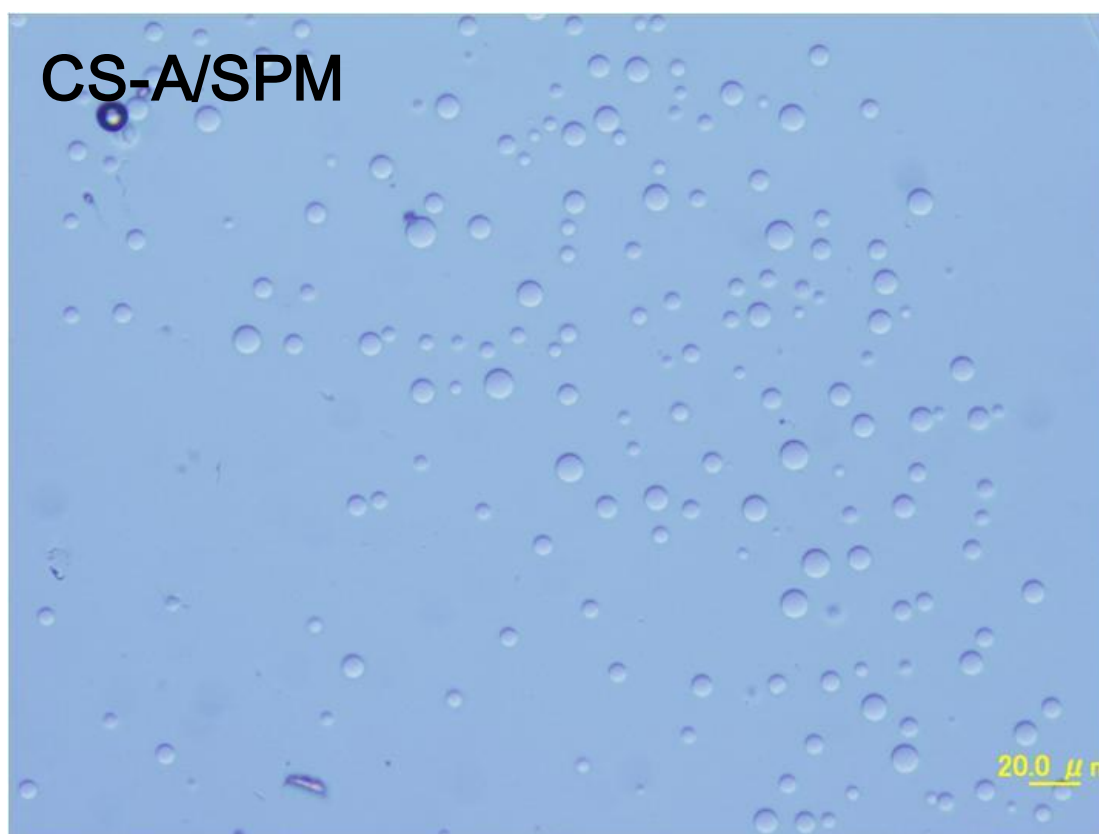


**Fig. 1-7 Microscopic image of PIC generated from 15 kDa of CS and SPM.**

**The scale-bar indicates 20.0  $\mu\text{m}$ .**

**Table 1-1 The sizes and  $\zeta$ -potentials of PIC particles generated under the optimal mixing ratio conditions between CS and polyamines.**

PIC formation	MV ( $\mu\text{m}$ )	$\zeta$ (mV)
40 mg/mL of 15 kDa CS + 50 mM of SPM	3.41 $\pm$ 0.64	-0.80 $\pm$ 0.25
20 mg/mL of 8 kDa CS + 50 mM of SPM	2.95 $\pm$ 2.52	-9.94 $\pm$ 0.52
20 mg/mL of 5 kDa CS + 20 mM of SPM	1.64 $\pm$ 1.61	-1.96 $\pm$ 1.35
80 mg/mL of 46 kDa CS + 100 mM of SPM	4.17 $\pm$ 2.92	-11.82 $\pm$ 0.86
40 mg/mL of 15 kDa CS + 20 mM of Cdp	1.65 $\pm$ 0.53	-25.19 $\pm$ 1.03
80 mg/mL of 15 kDa CS + 20 mM of Cdh	2.00 $\pm$ 1.26	-32.93 $\pm$ 0.47
40 mg/mL of 15 kDa CS + 20 mM of Taa	0.42 $\pm$ 0.16	-34.67 $\pm$ 1.15

Mean  $\pm$  SD,  $n = 3$ .

Fig. 1-8 shows the generation scheme of PIC by mixing CS and SPM. We considered that SPM and CS combined with each other by the electrostatic interaction between amino groups in SPM and sulfo groups and carboxyl groups in CS.

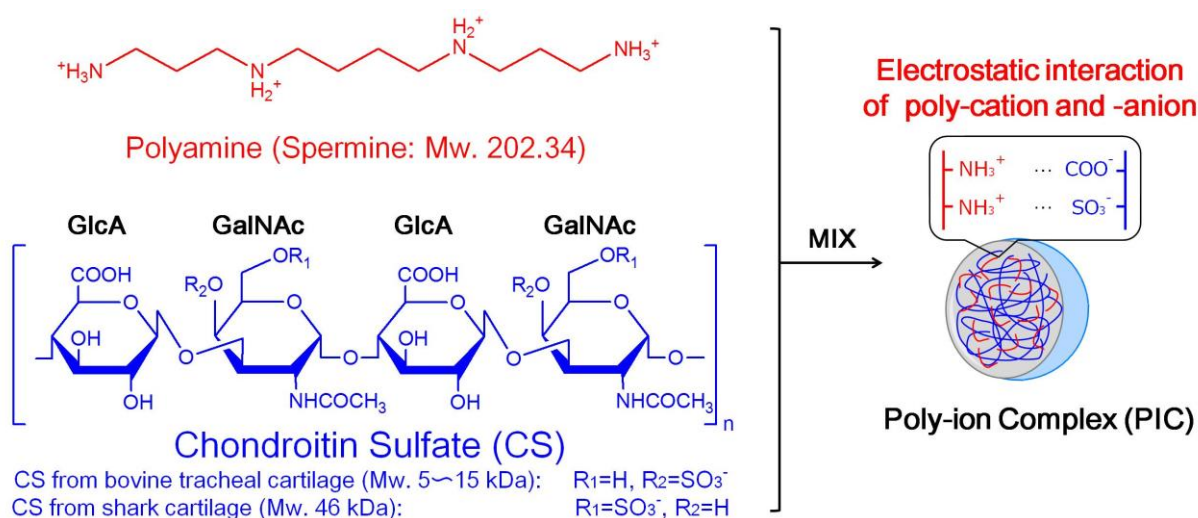


**Fig. 1-8 The generation scheme of poly-ion complex (PIC) by SPM and CS.**

### 1.3.2. Effect of Mixing Concentration Ratio Between CS and SPM on PIC Formation Efficiency

To understand the properties of PIC, the PIC formation efficiency was firstly investigated under different mixing ratios of CS and SPM concentrations. We evaluated the PIC formation efficiency by turbidimetric measurement at 600 nm, namely to determine the % transmittance ( $T$ ) using spectrophotometer. The PIC formation efficiency was separated into 5 grades and representative examples for each evaluation level were presented in Fig. 1-9-1: -, PIC formation could not be observed ( $\geq 90\%T$ ); +, PIC formation was poor ( $30\sim 89\%T$ ); ++, PIC formation was good ( $10\sim 29\%T$ ); +++, PIC formation was very good ( $1\sim 9\%T$ ) and after 24 h still exhibited

strongly turbid white solution; +++++, PIC formation was the best of all conditions (<1% *T*) but PIC precipitated very quickly (within several seconds). The transmittances for the representative examples were 99.2% *T* (-), 30.6% *T* (+), 11.8% *T* (++), 3.2% *T* (+++) and 0.6% *T* (++++), respectively.

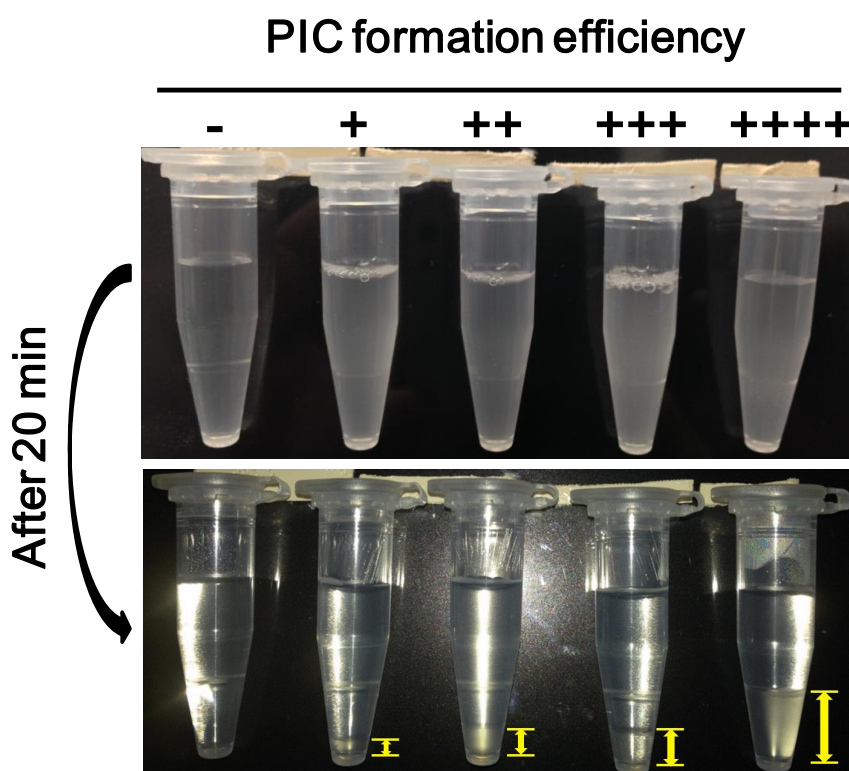


**Fig. 1-9-1 Representative instances for each evaluation level of PIC formation efficiency.**

15 kDa of CS and SPM were separately dissolved in double-distilled water at different concentrations, and then same volumes of CS solution and SPM solution were well mixed with one another to generate PIC. As the result shown in Fig. 1-9-2, the PIC generated from 40 mg/mL of 15 kDa CS and 50 mM of SPM possessed the optimal formation efficiency. PIC formed by higher or lower concentration of CS didn't have so good formation efficiency as this mixing condition. Similarly, SPM at

higher or lower concentration also did not avail the PIC formation. Therefore, it was demonstrated that the mixing ratio of CS and SPM was one important factor that affected the PIC formation efficiency. And this optimized PIC condition was used for the next experiment.

		SPM·4HCl			
		10 mM	20 mM	50 mM	100 mM
CS (bovine tracheal cartilage) Mw. 15 kDa	10 mg/mL	+	++	++	+
	20 mg/mL	+	++	++	++
	40 mg/mL	-	++	+++	++
	80 mg/mL	-	-	++	++
	200 mg/mL	-	-	-	-

**Fig. 1-9-2 PIC formation efficiencies under different conditions of mixing concentration ratio between 15 kDa CS and SPM.**

### 1.3.3. Effect of pH Value on PIC Formation Efficiency

Next, the effect of pH value on the optimized PIC sample was examined under various pH conditions. Based on our previous results, the PIC formation could not be observed under strongly basic conditions ( $\text{pH} > 11$ ) (data not shown). Therefore, the purified PIC particles that were generated under diverse pH conditions were dissociated by the addition of sodium hydroxide, and then SPM was separated from CS using 10 K cut-off spin columns. The resulting free CS and SPM were quantitatively determined by HPLC for calculating the ratio of their contents that were combined in PIC under different pH conditions (Fig. 1-10). The experiments were repeated twice with reproducible results. Consequently, it was observed that the PIC formation efficiency was the highest at pH 6.0. Supposing the molecular weight of CS is uniform, we are able to calculate that approximately 10 molecules of SPM

(correspond to 40 positive charges) bound to one molecule of 15 kDa (dp30) of CS (correspond to 60 negative charges). The observation that weakly acidic conditions are most suitable for the PIC formation can be explained by the combination ratio between 40 positive charges from amino groups of SPM (4 amino groups /SPM  $\times$  10 mol) , and 60 negative charges from sulfo and carboxyl groups of CS (2 negative charges /disaccharide unit  $\times$  dp30). Moreover, this was also consistent with the analysis for the characteristic properties of PIC that the  $\zeta$ -potential was  $-0.80 \pm 0.25$  mV (Table 1-1).

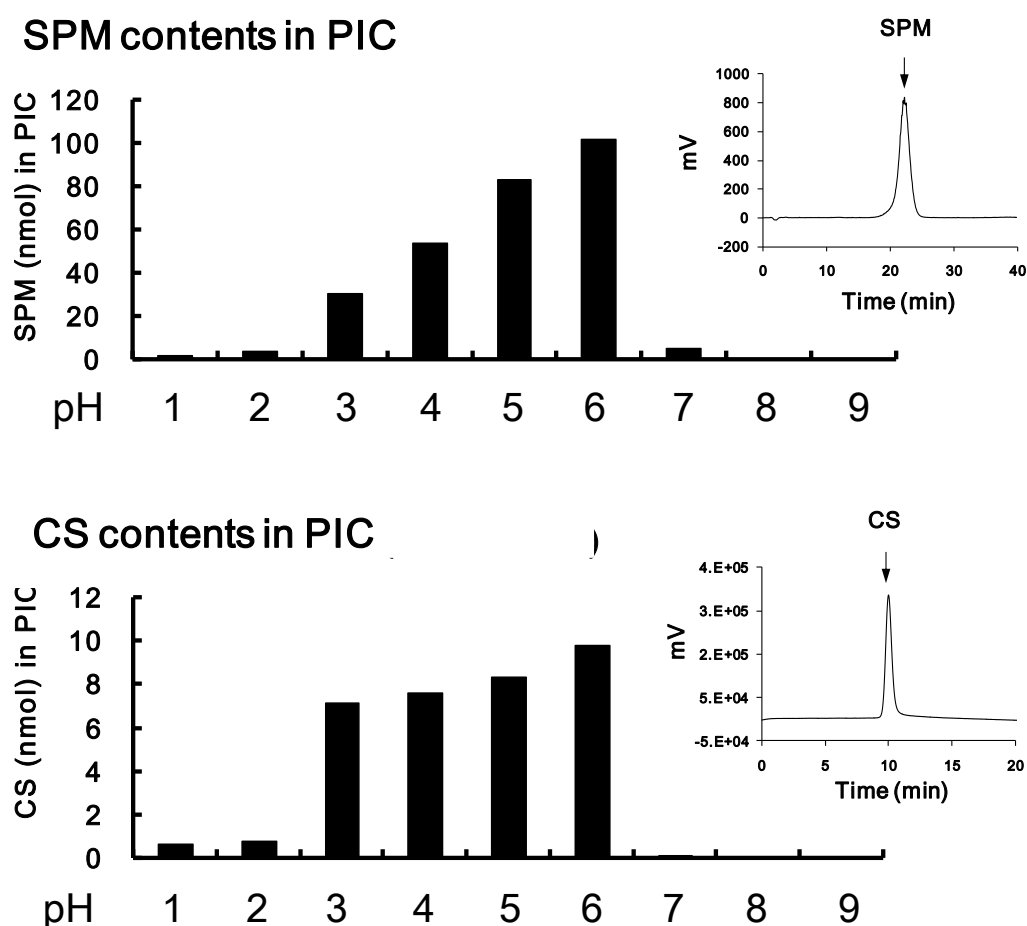


**Fig. 1-10** The contents of SPM and 15 kDa of CS in PIC at diverse pH values.

### 1.3.4. Effect of the Molecular Size of CS on PIC Formation Efficiency

LMWCS with molecular weight of 8 kDa and 5 kDa were gained at the reaction time of about 7 and 15.5 h, respectively (Fig. 1-11-1). The chemical structure of LMWCS was confirmed by the  $^1\text{H}$ -NMR spectra (Fig. 1-11-2). It was revealed that the characteristic proton NMR signals observed from 15 kDa CS were also confirmed from LMWCS spectrum. Therefore, it was declared that the sugar chain structure of CS was still retained after the photodegradation reaction. Moreover, the relative peak intensity at 4.9 ppm (GalNAc(4S) H-4) and 4.4 ppm (GalNAc(6S) H-6) almost kept unvaried, which demonstrated that the photodegradation method utilizing titanium dioxide to produce LMWCS scarcely caused desulfurization.

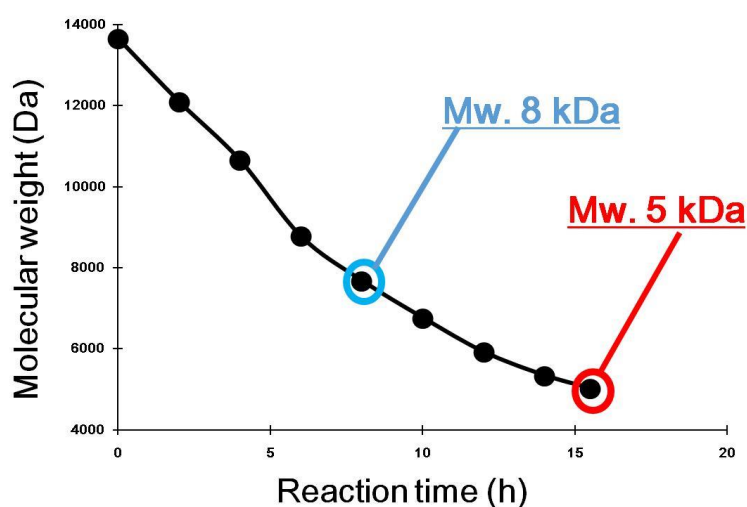


**Fig. 1-11-1** Molecular weight of LMWCS at different light exposure time.

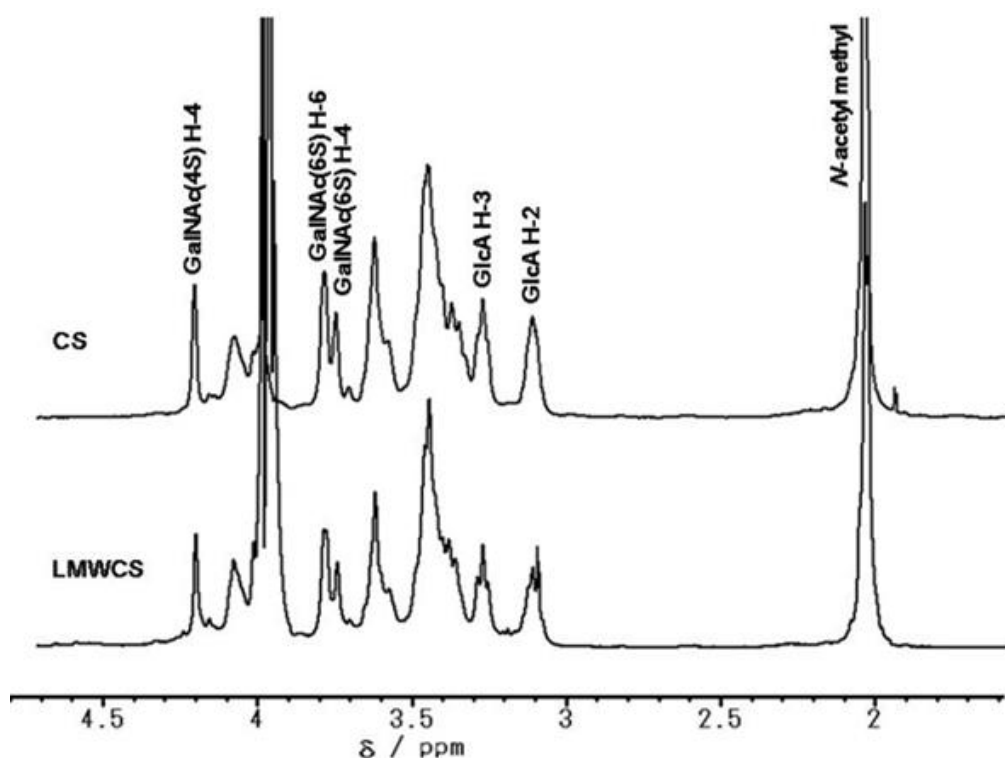


**Fig. 1-11-2 One-dimensional  $^1\text{H}$ -NMR spectra (400 MHz) of CS-A and LMWCS.**

The effect of molecular weight of CS on PIC formation was investigated using 46 kDa, 8 kDa and 5 kDa CS. These CS samples were similarly dissolved in water and the conditions to generate a maximum PIC with SPM were explored. As a result, the optimal conditions for PIC formation were different among the various chain lengths of CSs (Fig. 1-12). Moreover, efficiency of PIC formation behaved in a CS molecular weight-dependent manner. CS with lower molecular size almost did not form PIC, while CS with higher molecular weight was more effective for the PIC generation. Similarly to PIC formed by 15 kDa CS, the spherical PIC particles generated from LMWCS were also observed when PIC solutions were adequately mixed. The size and shape of PIC could not be maintained for long time because adjacent PIC particles were extremely prone to merging with one another (data not shown). Especially, we noticed that 46 kDa of CS generated considerable PICs, however these PIC particles precipitated very quickly within several seconds.

Interestingly, the surface charges of PIC coming from 8 kDa or 46 kDa of CS were significantly different from those of PIC generated by 15 kDa or 5 kDa of CS despite an almost identical particle size of PIC (Table 1-1). In contrast with the  $\zeta$ -potentials of the PICs, coming from 15 kDa and 5 kDa of CS, being near 0 mV, the PICs formed using 8 kDa and 46 kDa of CS showed  $\zeta$ -potentials around -10 mV.

		SPM-4HCl			
		10 mM	20 mM	50 mM	100 mM
Low Molecular Weight CS Mw. 5 kDa	10 mg/mL	+	+	-	-
	20 mg/mL	-	++	+	-
	40 mg/mL	-	-	+	-
	80 mg/mL	-	-	-	-
	200 mg/mL	-	-	-	-
		SPM-4HCl			
		10 mM	20 mM	50 mM	100 mM
Low Molecular Weight CS Mw. 8 kDa	10 mg/mL	+	+	+	-
	20 mg/mL	+	+	++	-
	40 mg/mL	-	+	+	-
	80 mg/mL	-	-	-	-
	200 mg/mL	-	-	-	-
		SPM-4HCl			
		10 mM	20 mM	50 mM	100 mM
CS (shark cartilage) Mw. 46 kDa	10 mg/mL	+	+	+	+
	20 mg/mL	+	++	++	+
	40 mg/mL	-	+	+	+++
	80 mg/mL	-	-	+	++++
	200 mg/mL	-	-	-	-

**Fig. 1-12 Effect of the molecular weight of CS on the PIC formation efficiency.**



### 1.3.5. Effect of Unusual Polyamines on PIC Formation Efficiency

It has been known that thermophilic bacteria and *archaea* are a rich source of a wide variety of unusual polyamines. In particular, an extreme thermophile (*eubacterium*), *Thermus thermophilus*, produces various kinds of unusual polyamines such as caldopentamine (Cdp), caldohexamine (Cdh), tris (3-aminopropyl) amine (Mitsubishine) and tetrakis (3-aminopropyl) ammonium (Taa) (Fig. 1-5).<sup>28)</sup> Since unusual polyamines, especially Taa, stabilize ssDNA and tRNA more effectively than SPM, the effect of the unusual polyamines on PIC formation with 15 kDa of CS was examined under lower concentration conditions. As displayed in Fig. 1-13-1, the optimal conditions of PIC formations were various among the unusual polyamines. Particularly, Mitsubishine was unable to form PIC with 15 kDa of CS, in contrast to the strong PIC formation observed for well mixed by the equivalent volumes of 40 mg/mL of 15 kDa CS and 20 mM Taa. Although amount of the resulting PIC particles coming from Taa was almost equal to that from SPM after the PIC solutions separated into layers, the configuration and the color of the PIC generated by Taa was obviously different (Fig. 1-13-2). Furthermore, it was observed that PIC coming from Taa maintained its particle size for a relatively longer time (more than 1 h) and the particles did not quickly merge into one another (Fig. 1-13-3). The particle size of the PIC formed by Taa was the smallest ( $0.42 \pm 0.16 \mu\text{m}$ ) among all the PICs examined, however, Taa afforded the lowest  $\zeta$ -potential value ( $-34.67 \pm 1.15 \text{ mV}$ ) (Table 1-1). The reason for this may be because Taa can bind to CS more effectively than any of the other polyamines.<sup>28)</sup>

		Caldopentamine·5HCl (Cdp·5HCl)				
		1 mM	2 mM	5 mM	10 mM	20 mM
CS (bovine tracheal cartilage) Mw. 15 kDa	20 mg/mL	-	-	-	+	+
	40 mg/mL	-	-	-	-	++
	80 mg/mL	-	-	-	-	-

		Caldohexamine·6HCl (Cdh·6HCl)				
		1 mM	2 mM	5 mM	10 mM	20 mM
CS (bovine tracheal cartilage) Mw. 15 kDa	20 mg/mL	-	-	+	+	+
	40 mg/mL	-	-	-	+	+
	80 mg/mL	-	-	-	-	++

		Tris(3-aminopropyl)amine·4HCl (Mitsubishine·4HCl)				
		1 mM	2 mM	5 mM	10 mM	20 mM
CS (bovine tracheal cartilage) Mw. 15 kDa	20 mg/mL	-	-	-	-	-
	40 mg/mL	-	-	-	-	-
	80 mg/mL	-	-	-	-	-

		Tetrakis(3-aminopropyl)ammonium·5HCl (Taa·5HCl)				
		1 mM	2 mM	5 mM	10 mM	20 mM
CS (bovine tracheal cartilage) Mw. 15 kDa	20 mg/mL	-	-	+	++	+
	40 mg/mL	-	-	-	+	+++
	80 mg/mL	-	-	-	-	+

Fig. 1-13-1 Effect of unusual polyamines on the PIC formation efficiency.

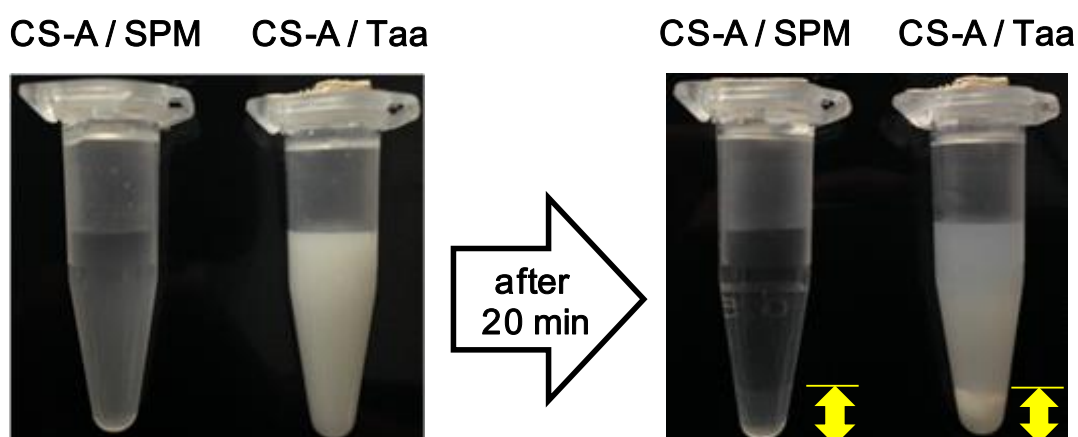
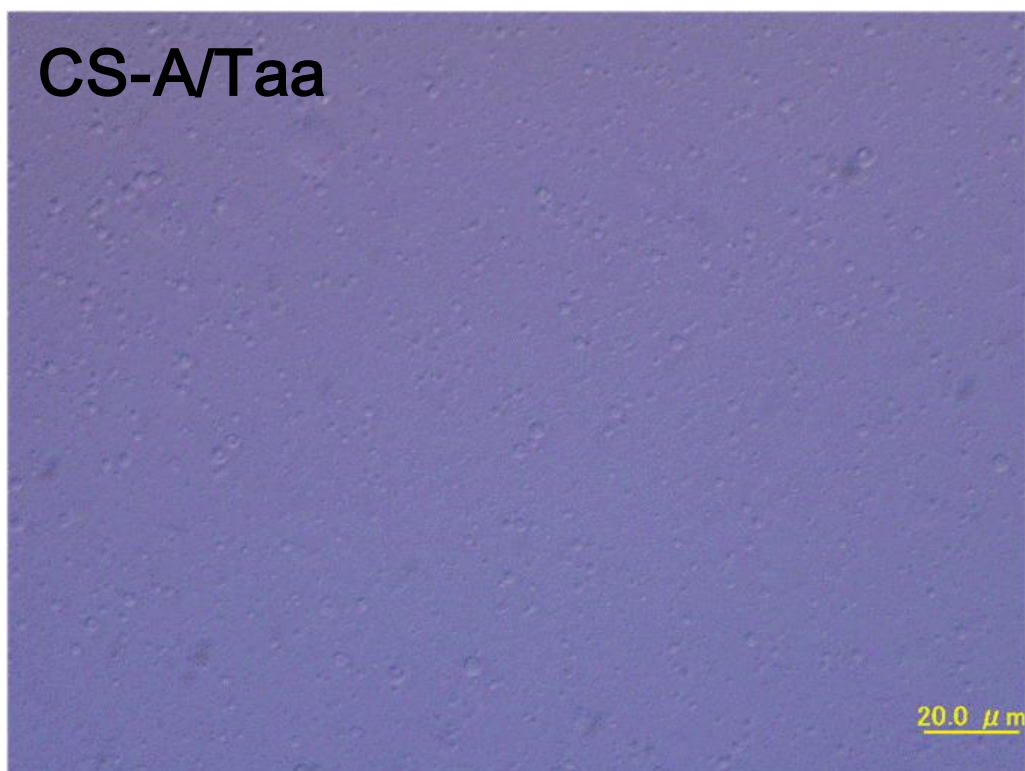


Fig. 1-13-2 Photographs of the PIC (15 kDa CS-A+SPM) and PIC (15 kDa CS-A+Taa).



**Fig. 1-13-3 Microscope image of PIC generated from 15 kDa of CS and Taa.**

**The scale-bar indicates 20.0  $\mu\text{m}$ .**

It is thought that the maintenance of PIC particle size is an important factor to improve the absorption efficiency of the PIC in gastrointestinal tract. In general, CS chains may exist as a linear form in neutral pH and the electrostatic repulsion of each sulfonate/carboxyl group of CS chain must affect their coagulation. However, once some parts of negatively charged acidic groups of CS were electronically neutralized by amines, it might be allowed to change their forms in solution as a complex. As mentioned above, PIC formations by the combination of CS (5 kDa, 8 kDa, 15 kDa and 46 kDa) and linear polyamines such as SPM, Cdp and Cdh were successfully conducted. However, their particles were extremely prone to merging with one another. It is conceivable that PIC particles obtained by the electrical attachment of linear polyamines to linear CS in the parallel positions are unable to keep their size. In the case of branched polyamines, Taa and Mitsubishine showed different PIC

formation with linear CS. Especially, Taa exhibited the generation of different type of PIC compared with any of the other polyamines, suggesting that Taa but not Mitsubishiine maybe caused the structural changes of CS (or bridge connection between CSs) and consequently maintained the PIC particle size. In the light of these observations, we speculate that maintenance of the size of PIC generated by CS and polyamines requires structural changes of CS based on the binding with branched polyamines possessing numerous positively charged amino groups. Experiments are in progress to develop the more stable PIC generation using branched polyamines.

### **1.3.6. Effect of PIC Formation on the Oral Intake of CS in Animal Models**

There have been several experiments evaluating the nanoparticles that have permeating activity into the epithelial cell layer.<sup>49-52)</sup> However, there are two issues for evaluation of PIC generated in this study. One is the toxicity of extracellular SPM because amine oxidase in fetal calf serum produces aminodialdehyde-generating acrolein.<sup>53)</sup> The other is the stability of PIC particles formed in this study, because adjacent PIC particles quite tended to come together and make one larger particle, which might influence the oral intake efficiency of PIC. For this reason, the effect of PIC formation on the oral intake of CS was directly evaluated *in vivo*.

Under our experimental conditions, orally absorbed CS was observed in the plasma of only one mouse in the total 7 mice (14.3% of mice) without any injury caused by scratching in the 15 kDa CS (500 mg CS/kg body weight) dosed group (Fig. 1-14a). In the case of colitis model mouse, induced by dextran sulfate,<sup>54)</sup> a significant level of 15 kDa of CS was absorbed by the inflamed colon (data not shown), while we did not find any inflammation in intestine or colon of mice in this study by surgical operation after the experiments. Subsequently, PIC was orally administered to mice at a single dose of 500 mg CS/kg body weight and the plasma concentration—time profiles of CS were plotted (Fig. 1-14b). CS concentration in plasma increased in 4

mice in the total 9 mice (44.4% of mice) when PICs, generated from 15 kDa of CS and SPM, were treated to mice. Generally, a lower molecular weight CS is regarded as better absorbed than a greater CS, however, the PICs generated from 8 kDa and 5 kDa CS almost did not help increase the CS oral absorption efficiency (Figs. 1-14c and d). Moreover, the effective absorption of PIC formed by 46 kDa CS and SPM or PIC generated by 15 kDa CS and Taa was hardly observed (Figs. 1-14e and f).

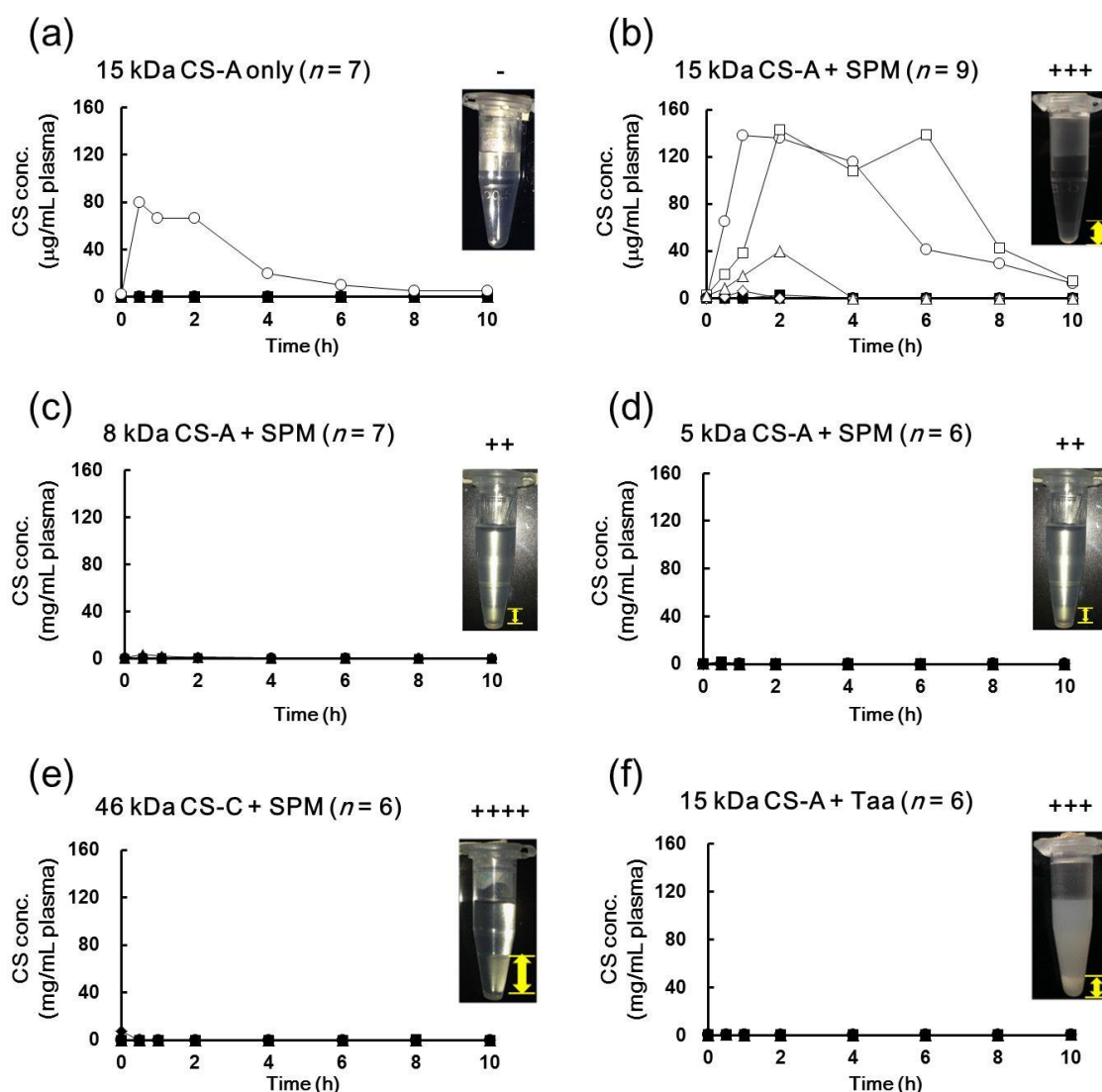


**Fig. 1-14 Effect of PIC formation on the oral intake of CS in mice.**

CS contents in the plasma of mice orally administrated with CS alone or PIC were determined following the “Experimental”. Each profile represents one mouse.

To better understand the absorption of PIC, the  $\zeta$ -potentials of various kinds of PIC particles were subsequently determined under their corresponding mixing ratio conditions for the best PIC formation efficiency. As a result, the PIC generated by 15 kDa of CS and SPM possessed nearly electrically neutral particle surface charges, while other PIC particles (except for the mixing ratio condition of 5 kDa CS and SPM) were negatively surface charged (Table 1-1 and Fig. 1-15).

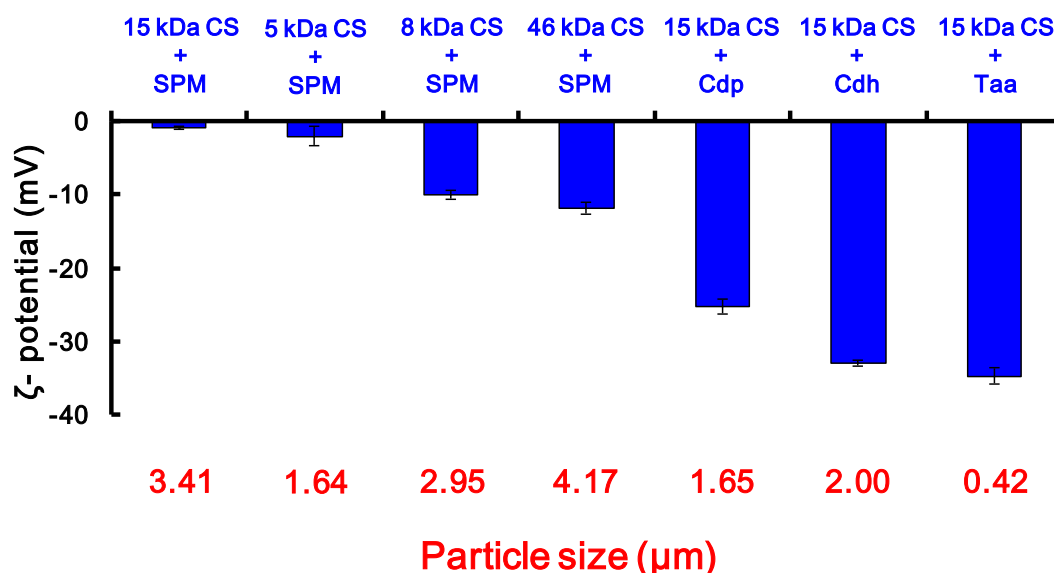


**Fig. 1-15 The determination of PIC particle size and surface charge.**

If PIC having neutral surface charge is critical for the absorption in gastrointestinal tract, it is important to better understand the condition of PIC derived from various length of CS. In the case of 15 kDa CS (dp30), we determined that approximately 10 molecules of SPM (correspond to 40 positive charges) bound to one molecule of 15 kDa CS (correspond to 60 negative charges) when CS (40 mg/mL) and SPM (50 mM) were mixed (Fig. 1-10). If the mixing ratio between the number of anionic groups in CS (5 kDa, 8 kDa or 46 kDa) and that of cationic groups in SPM

also obeyed this ratio between 15 kDa CS (40 mg/mL) and SPM (50 mM), similar PICs having nearly neutral surface charges were obtained (Table 1-2). The  $\zeta$ -potentials of PIC particles generated by 40 mg/mL of various lengths of CSs and 50 mM SPM were  $-3.12 \pm 8.96$  mV (5 kDa CS),  $-2.96 \pm 2.35$  mV (8 kDa CS) and  $-3.62 \pm 0.54$  mV (46 kDa CS), respectively. However, it should be noted that PIC amounts obtained under these conditions were less, compared with the optimal mixing ratio conditions (Fig. 1-12). In the case of 5 kDa CS, the mixing condition of 20 mg/mL of 5 kDa CS + 20 mM SPM also afforded the PIC having nearly neutral surface charge (Table 1-1), however, substantial absorption was not observed (Fig. 1-14d), which was probably due to the lower PIC formation efficiency. These results indicate that the high formation efficiency and electrically neutral surface charge of PIC particles are both important factors for their effect on oral CS bioavailability.

**Table 1-2. The  $\zeta$ -potential of PIC particles generated under the mixing ratio condition of negative charges in CS : positive charges in poliamines = 60 : 40.**

PIC formation	$\zeta$ (mV)
40 mg/mL of 5 kDa CS + 50 mM of SPM	$-3.12 \pm 8.96$
40 mg/mL of 8 kDa CS + 50 mM of SPM	$-2.96 \pm 2.35$
40 mg/mL of 46 kDa CS + 50 mM of SPM	$-3.62 \pm 0.54$

Mean  $\pm$  SD,  $n = 3$ .

Unfortunately, it was yet unclear why the detected amounts of CS, which was absorbed in the oral PIC form, were so uneven in plasma samples of individual mice (Fig. 1-14b). We assume that under the physiological conditions in the intestine (pH 7 ~ 8), the PIC particles probably will be dissociated according to the results from Fig.

1-10, which may be one reason that inhibits the PIC oral absorption. Furthermore, the PIC particles formed by CS and SPM are unstable and easily merge with one another, possibly also influencing the oral intake efficiency of PIC.

In light of these observations, the more stable PIC particles simultaneously possessing high formation efficiency and neutral surface charges might represent a promising core structure for further development of oral CS delivery system.

#### **1.4. Summary**

The formation of PIC was found through the electrostatic interaction between CS and polyamines in water solutions. Thus, the physicochemical properties of PICs were investigated in the aqueous phase. It was demonstrated that the efficiency of PIC formation was influenced by various factors including the mixing concentration ratio of CS and polyamines, the molecular weight of CS, the nature of polyamines and pH value. The optimal PIC sample generated from 15 kDa of CS and SPM was the most stable at pH 6.0 and combining molar ratio of CS : SPM was 1 : 10. This PIC formation afforded a particle size of  $3.41 \pm 0.64 \mu\text{m}$  and a  $\zeta$ -potential of  $-0.80 \pm 0.25 \text{ mV}$ . Furthermore, based on the *in vivo* experiments, the PIC generated from SPM and 15 kDa of CS had the best absorption by oral administration when compared to CS alone or other PICs. PICs generated by 15 kDa of CS and Taa were the most stable PICs with particle size of  $0.42 \pm 0.16 \mu\text{m}$ , despite their undesirable negative  $\zeta$ -potential. In conclusion, PIC utilizing polyamines appears to be a promising core structure for the development of CS delivery system. The high formation efficiency and electrically neutral surface charge of PIC particles are both important factors for their effect on oral CS bioavailability.



## Chapter 2

### The formation and characterization of poly-ion complex generated through the interaction between heparin and polyamines

#### 2.1. Introduction

Heparin (HP), another member of the GAG family, consists of a ( $\alpha$  1 $\rightarrow$ 4) linked repeating disaccharide unit that is composed of glucuronic acid or iduronic acid along with glucosamine. Unfractionated heparin is a heterogeneous polydispersed mixture of sulfated polysaccharides substituted with *O*-sulfo groups or *N*-sulfo groups at different positions. The molecular weight of heparin ranges from 3 kDa to 30 kDa with an average molecular mass of 15 kDa.<sup>15-17)</sup> Heparin is widely used as an anticoagulant in the clinical researches and can bind to the serine protease inhibitor antithrombin (AT), causing it to undergo a conformational change resulting in AT inhibition of thrombin (Factor IIa) and Factor Xa. AT binds to the specific pentasaccharide sequence [GlcNAc6S (1 $\rightarrow$ 4) GlcA (1 $\rightarrow$ 4) GlcNS3S6S (1 $\rightarrow$ 4) IdoA2S (1 $\rightarrow$ 4) GlcNS6S)] in heparin (Fig. 2-1).<sup>46,55)</sup> However, similarly to CS, the oral bioavailability of heparin is pretty low because of its high molecular weight (3~30 kDa) and the highest negative charge density of any known biological molecule. Accordingly, heparin is only used as intravenous or subcutaneous injection but not preparation for oral use, which severely limits its application.

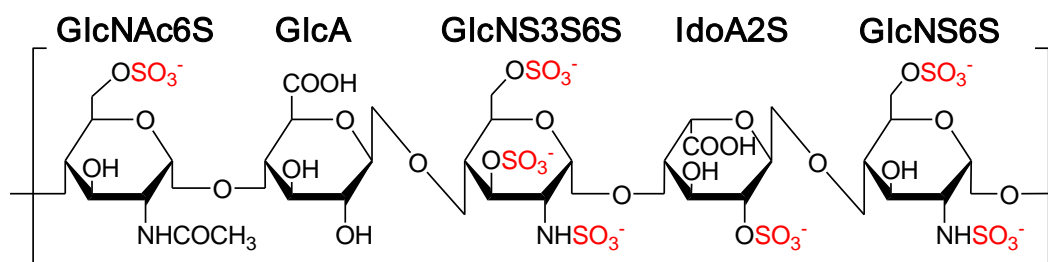


Fig. 2-1 The pentasaccharide sequence in heparin that binds to antithrombin.

There have been several reports demonstrating that the conjugation of hydrophobic bile acids with low molecular weight heparin (LMWHP) allowed effective absorption in the intestine through binding with bile acid transporter found on the apical epithelial cell membrane.<sup>49-52)</sup> In the clinical researches, unfractionated heparin exhibits some undesirable side effects. Thus, low molecular weight heparin, with sustained antithrombotic activity, more predictable pharmacological action, and better bioavailability,<sup>18,56-58)</sup> has been introduced as heparin substitute for reduced side effects. The most common commercially available LMWHP includes Enoxaparin, Dalteparin and so on.

Under the inspiration of poly-ion complex (PIC), in this study we attempted to mix heparin and natural polyamines in aqueous solutions. Similarly to CS, the formation of turbid white PIC was also found through the electrostatic interaction between heparin and polyamines in water solutions and we also investigated whether the generated PIC effected on heparin oral absorption or not.

## **2.2. Experimental**

### **2.2.1. Chemicals and Materials**

Heparin (average molecular weight: 20 kDa, extracted from porcine intestine) was purchased from New Zealand Pharmaceutical Co., Ltd. Putrescine dihydrochloride (PUT·2HCl), Spermidine trihydrochloride (SPD·3HCl) and Spermine tetrahydrochloride (SPM·4HCl) were obtained from Nacalai Tesque Inc. (Kyoto, Japan). The heparin assay kit containing Factor Xa, Normal human plasma, Antithrombin III and the coloring synthetic substrate S-2222 was purchased from Test Team Heparin S<sup>®</sup>, Sekisui Medical Co., Ltd (Tokyo, Japan). Water used in studies was

purified using Q-GARD<sup>®</sup> 1, Millipore. All other chemicals were of analytical reagent grade and used without further purification.

### **2.2.2. PIC Formation**

Similarly to case of CS, heparin and polyamines were separately dissolved in double-distilled water, with a doubled concentration of the target PIC, and then equivalent volumes of heparin solution and polyamine solution were fully mixed with each other to generate PIC. PIC formation efficiency was evaluated by turbidimetric measurement at 600 nm, namely the determination of % transmittance ( $T$ ), using thermo scientific SPECTONIC 20D+ digital spectrophotometer, and was expressed as -, +, ++ and so on same as Chapter 1.

### **2.2.3. Effect of Mixing Concentration Ratio Between Heparin and Polyamines on PIC Formation Efficiency**

To understand the effect of mixing ratio between heparin and polyamines on PIC generation, the PIC formation efficiencies were evaluated under different mixing concentration ratio conditions between 20 kDa of heparin extracted from porcine intestine and SPM/SPD/PUT.

### **2.2.4. The $\zeta$ -Potential Determination**

Similarly to the case of CS, the  $\zeta$ -potential determination was performed for the PIC sample generated from heparin and polyamines on the ELS-Z1 (Otsuka Electronics Co., Ltd, Osaka, Japan) at the 60 V of voltage. Double-distilled water was used as the dispersant and the measurements were carried out at 25°C. The average of three measurements was taken as the final characteristic parameter.

### **2.2.5. Effect of PIC Formation on the Oral Intake of Heparin in Mouse Models**

All animal experiments were approved by the Institutional Animal Care and Use Committee of Chiba University and carried out according to the guidelines for Animal Research of Chiba University. The ddY mice (female, weighing 28 - 30 g, Japan SLC, Inc, Shizuoka, Japan) were housed at 25°C and 55% RH. A 12 h dark/light cycle was maintained throughout. Mice had free access to standard pellet diet (MF, Oriental Yeast Co., Ltd, Tokyo, Japan) and tap water, and were fasted overnight before the experiment, because it was considered that the diet might contain heparin and influence the experiment results. The solution containing fully mixed PIC or heparin alone was orally administered to each group (comprising 6 mice) at a single dose of 500 mg HP/kg body weight (*ca.* 15 mg HP/each animal). Blood samples were collected from the tail vein at time intervals of 0, 0.5, 1, 2, 3, 4, 6 h after oral administration and were anticoagulated with 3.2% trisodium citrate solution at the ratio of blood : 3.2% trisodium citrate = 9 : 1. Each collected sample was immediately centrifuged at 800 g for 15 min to obtain the plasma, which was transferred to a new Eppendorf tube and stored in a deep freezer until used. The schedule of oral administration of PIC in animal models was similar to Fig. 1-3 described previously with minor modifications.

### **2.2.6. Determination of Heparin Contents in Mouse Plasma**

The contents of heparin that were absorbed into the mouse plasma *via* oral route were determined by the Anti-Factor Xa Activity Assay using heparin assay kits.

#### **Preparation of Standard Solutions**

Clexane kit for subcutaneous injection (2000 IU/0.2 mL) was utilized as the standard sample. The standard sample was firstly diluted to 10 IU/mL with 0.9% NaCl

solutions and then further diluted to 0.2 IU/mL with Tris buffer (pH 8.4). 0/20/40/60/80  $\mu\text{L}$  of the diluted standard samples were dissolved with 160/140/120/100/80  $\mu\text{L}$  of Tris buffer (pH 8.4), respectively, and then 20  $\mu\text{L}$  of 1 U/mL ATIII and 20  $\mu\text{L}$  of normal human plasma were serially added to each sample. Thus, 0/0.2/0.4/0.6/0.8 IU/mL plasma of standard solutions was acquired for plotting the calibration curve.

### **Preparation of Specimen Solutions**

5  $\mu\text{L}$  of each collected mouse plasma sample was diluted with 15  $\mu\text{L}$  of the normal human plasma and then dissolved with 160  $\mu\text{L}$  of Tris buffer (pH 8.4), followed by the addition of 20  $\mu\text{L}$  of 1 U/mL ATIII. The final 200  $\mu\text{L}$  of specimen solution was obtained for determination (Fig. 2-2).

### **Determination**

As shown in Fig.2-2, 200  $\mu\text{L}$  of the standard solutions or specimen solutions were incubated at 37°C for 5 min and then added with 100  $\mu\text{L}$  of 7.1 nkat/mL factor Xa solution that was excessive for the reaction. After incubation at 37°C for exact 30 seconds, 200  $\mu\text{L}$  of 0.75 mg/mL S-2222 solution was added as the substrate to react with the excessive factor Xa at 37°C for 3 min. Subsequently, 300  $\mu\text{L}$  of 50% acetic acid was added to stop the reaction and the production of free p-nitroaniline was detected for the absorbance at 405 nm using TECAN Austria GmbH Sunrise Thermo (made in Austria). The calibration curve was constructed using the anti-factor Xa activity of standard solutions (IU/mL plasma) plotted against absorbance and the anti-factor Xa activity of each specimen was calculated from this calibration curve.

<b>Plasma</b>	5 $\mu$ L
— add normal human plasma	15 $\mu$ L
— add Tris buffer (pH 8.4)	160 $\mu$ L
— add anti-thrombin III	20 $\mu$ L
<b>Specimen</b>	200 $\mu$ L
<b>Specimen or Standard</b>	200 $\mu$ L
<b>Incubation at 37°C for 5 min</b>	
— add factor Xa	100 $\mu$ L
<b>Incubation at 37°C for 30 s</b>	
— add substrate (S-2222)	200 $\mu$ L
<b>Incubation at 37°C for 3 min</b>	
— add 50% acetic acid	300 $\mu$ L
<b>Determine the absorbance at 405 nm</b>	

**Fig. 2-2 Procedures for determination of anti-factor Xa activity.**

## **2.3. Results and Discussion**

### **2.3.1. Preparation of Poly-ion Complex**

Similarly to the case of CS, in this study we also firstly examined whether polyamine SPM could aggregate with the glycosaminoglycan heparin obtained from porcine intestine with an average molecular weight of 20 kDa. As the result shown in

Fig.2-3, the aqueous solution containing heparin (20 mg/mL) or SPM (20 mM) was clear and transparent, however, the turbid white PIC solution was generated when the equivalent volume of heparin and SPM solution were adequately mixed with one another. And after being settled for about 20 min, the turbid white solution separated into two layers. The upper layer was the water phase, and the lower layer was the PIC phase. Furthermore, the deposited PIC solution was restored back to a uniform solution after being thoroughly mixed again using vortex mixer. Similarly, we considered that PIC was generated through the electrostatic interaction between cationic groups in polyamines and anionic groups in heparin.

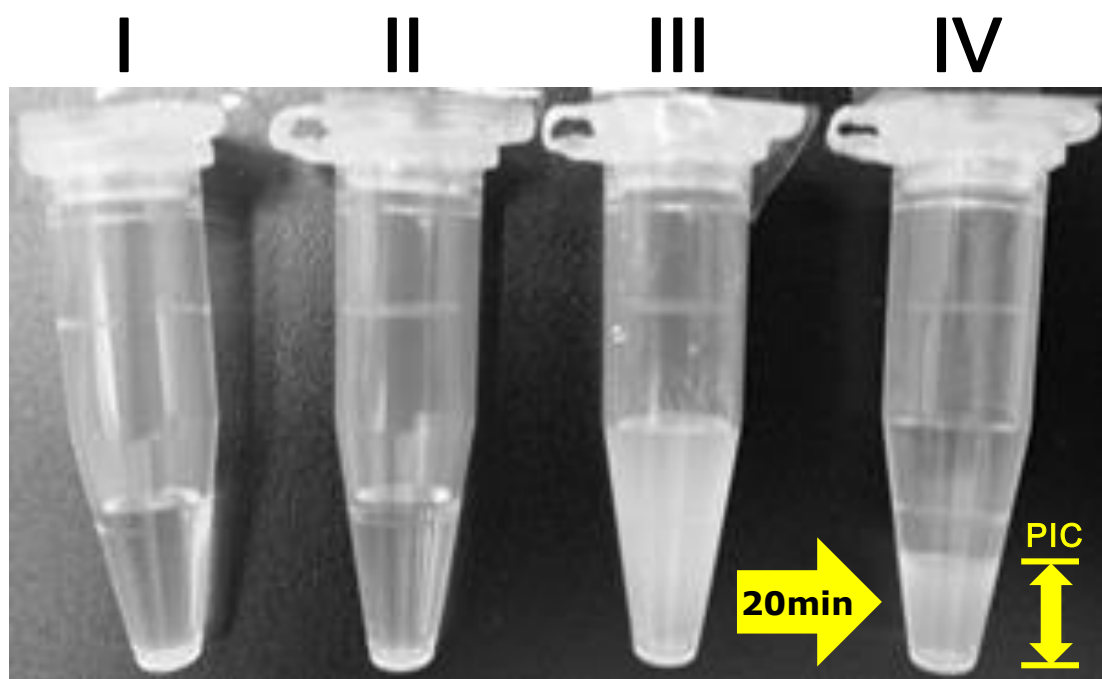


**Fig. 2-3 Photographs of (I) 20 mg/mL of Heparin, (II) 20 mM of SPM, (III) PIC, (IV) PIC that separated into two layers after standing for about 20 min.**

### 2.3.2. Effect of Mixing Concentration Ratio Between Heparin and Polyamines on PIC Formation Efficiency

20 kDa of heparin and SPM/SPD/PUT were separately dissolved in double-distilled water at different concentrations, and then same volumes of heparin solution and polyamine solution were well mixed with each other by different mixing concentration ratios to generate PIC. The PIC formation efficiency was evaluated as Fig. 1-9-1. Consequently, it was found that the PIC generated from 20 mg/mL of heparin and 20 mM of SPM afforded the best formation efficiency among various cases (Fig. 2-4). Heparin with too low concentration was not able to form PIC and the polyamines possessing more positive charges could facilitate the PIC formation. This indicated that mixing concentration ratio between heparin and polyamines, as a matter of fact, the mixing ratio between the number of anionic groups in heparin and that of cationic groups in polyamines, significantly affected the PIC formation efficiency.

		SPM·4HCl			SPD·3HCl			PUT·2HCl		
		20 mM	100 mM	200 mM	20 mM	100 mM	200 mM	20 mM	100 mM	200 mM
HP	0.02 mg/mL	-	-	-	-	-	-	-	-	-
	0.2 mg/mL	-	-	-	-	-	-	-	-	-
	1 mg/mL	+	+	+	+	+	+	-	-	-
	2 mg/mL	+	++	+	++	+	+	-	-	-
	10 mg/mL	++	++	++	+	+	+	-	-	-
	20 mg/mL	+++	++	++	-	-	++	-	-	-

**Fig. 2-4 PIC formation efficiencies under different conditions of mixing concentration ratio between 20 kDa heparin and polyamines.**



### 2.3.3. Effect of PIC Formation on the Oral Absorption of Heparin in Animal Models

The effect of PIC on the oral intake of heparin was examined in mouse models. Similarly to CS, the solution containing PIC or heparin alone was orally administered to mice and then the time course profiles were plotted for the heparin contents in mice blood plasma. However, it was regrettable that no mouse showed obvious heparin oral absorption in either the control group or the PIC dosed group (Fig. 2-5). In the clinical researches, the therapeutic range for heparin was considered to be around 0.5 IU/mL plasma anti-FXa activity (expressed as the red dotted line in Fig. 2-5). Thus, in this study the PIC formation did not assist to increase the oral heparin absorption at all.

Subsequently, we investigated the surface charge of the PIC sample and found that the  $\zeta$ -potential was  $-20.6 \pm 0.56$  mV. We considered that the extremely negative surface charge of the PIC particles could be one important reason that affected the heparin oral absorption.

It has been reported that the *N*-trimethyl chitosan coated polylactide-*co*-glycoside ( $\zeta$ -potential: around -10 mV) afforded the positive surface charges on the resulting nanoparticles and facilitated the oral absorption.<sup>59)</sup> Jain et al. also reported the preparation of cationic-coated liposome using polyallyl amine hydrochloride.<sup>60)</sup> These reports provide us with a promising approach for developing a cationic coating reagent for PIC generated from heparin and polyamines to ultimately improve the heparin bioavailability in the future study.

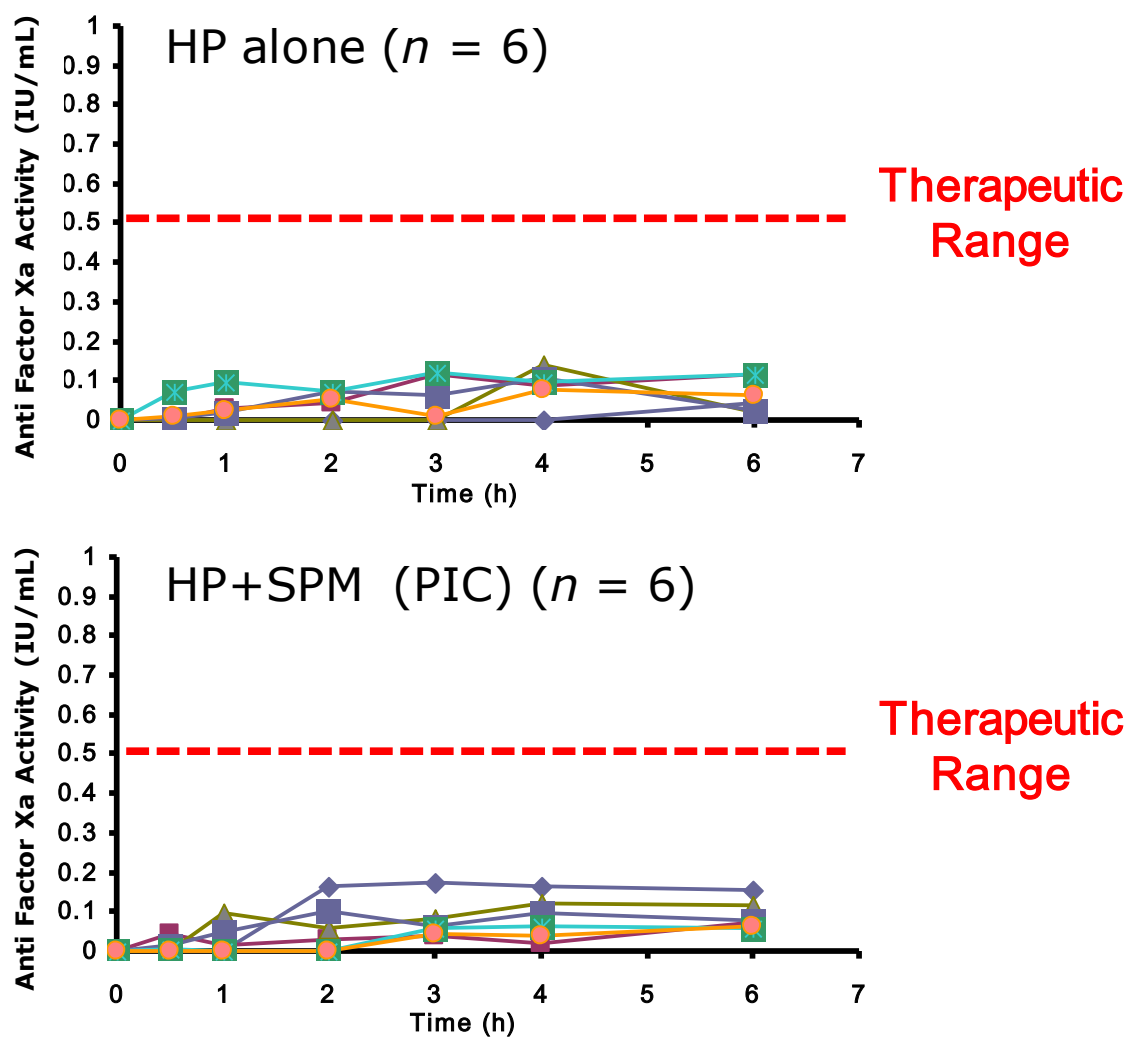


**Fig. 2-5 Effect of PIC formation on the oral intake of heparin in mice.**

Heparin contents in the plasma of mice orally administrated with heparin alone or PIC were determined following the “Experimental”. Each profile represents one mouse.

## 2.4. Summary

The formation of PIC was found by mixing heparin and polyamines in aqueous solutions. The PIC was considered to be generated through the electrostatic

interaction between cationic groups in polyamines and anionic groups in heparin. The PIC formation efficiency was significantly affected by the mixing concentration ratio between heparin and polyamines and 20 mg/mL heparin + 20 mM SPM afforded the optimal PIC formation among the three kinds of standard polyamines SPM/SPD/PUT. However, the *in vivo* experiments demonstrated that the PIC sample failed to increase the oral heparin absorption, probably because of the extremely negative surface charge of the PIC particles. Further researches are underway to develop the cationic-coated PIC for improving the heparin bioavailability through the gastrointestinal tract.

## Conclusion

In this study, we focused on the low oral bioavailability of glycosaminoglycans and therefore prepared poly-ion complex by mixing glycosaminoglycans and natural polyamines in aqueous solutions and investigated their effects on GAG absorption *via* the oral route. Chapter 1 and Chapter 2 aimed at the members of GAG family, chondroitin sulfate and heparin, respectively, and experiments were carried out for exploring the physicochemical properties and *in vivo* dynamic process of PICs generated from them.

### **Chapter 1 The formation and characterization of poly-ion complex generated through the interaction between chondroitin sulfate and polyamines**

#### **Preparation of poly-ion complex**

We observed that when the equivalent volume of transparent aqueous solutions containing CS and polyamines were fully mixed with one another, a turbid white solution of PIC was generated. We considered that polyamines and CS combined with each other by the electrostatic interaction between amino groups in polyamines and sulfo groups and carboxyl groups in CS.

#### **Physicochemical properties of PIC**

The physicochemical properties of PIC generated from CS and polyamines were investigated in the aqueous phase. It was demonstrated that the efficiency of PIC formation was influenced by various factors including the mixing concentration ratio of CS and polyamines, the molecular weight of CS, the nature of polyamines and pH value. The optimized PIC generated from 40 mg/mL of 15 kDa CS and 50 mM of SPM was the most stable at pH 6.0 and the combining molar ratio of CS : SPM was 1 : 10. This PIC formation afforded a particle size of  $3.41 \pm 0.64 \mu\text{m}$  and a  $\zeta$ -potential

of  $-0.80 \pm 0.25$  mV.

### **Effect of PIC formation on the CS oral intake in animal models**

Based on the *in vivo* experiments, the PICs generated from SPM and 15 kDa of CS got the best absorption by oral administration when compared to CS alone or other PICs. PICs generated by 15 kDa of CS and Taa were the most stable PICs with the smallest particle size, although the substantial absorption was not observed. According to the determination of  $\zeta$ -potential, we consider that the stable PIC particles simultaneously possessing high formation efficiency and electrically neutral surface charges might represent a promising core structure for further improvement of CS bioavailability in the digestive system.

## **Chapter 2 The formation and characterization of poly-ion complex generated through the interaction between heparin and polyamines**

### **Preparation of PIC**

Similarly to CS, the formation of turbid white PIC solution was observed after equivalent volumes of clear transparent heparin water solution and natural polyamines water solution were fully mixed with one another. We considered that PIC was generated through the electrostatic interaction between cationic groups in polyamines and anionic groups in heparin.

### **Effect of PIC formation on the heparin oral intake in animal models**

Similarly to CS, the solution containing PIC or heparin alone was orally administered to mice and then the time course profiles were plotted for the heparin contents in mice blood plasma. However, it was regrettable that the PIC formation did not help increase the oral heparin absorption, maybe because of the strongly negative surface charge of the PIC particles. Deeper studies are in progress to further improve the oral heparin bioavailability by developing the cationic-coated PIC.

## **Acknowledgements**

First and foremost, I would like to show my deepest gratitude to my supervisor, Professor Toshihiko Toida, a respectable, responsible and resourceful scholar, who has provided me with constructive suggestions and constant encouragements when I felt frustrated with the study. Without his enlightening instruction, impressive kindness and patience, I could not have completed my thesis. His keen and vigorous academic observation not only enlightens me in this thesis but also indicates a bright road in my future study.

Then, I would like to extend my sincere thanks to Associate Professor Kazuhiro Nishimura for his helpful guidance and valuable assistance throughout the course of this research.

I would also like to thank Assistant Professor Kyohei Higashi for his valuable guidance in every stage of the completion of this thesis. His kindness and the comprehensive knowledge he has taught me during the past three academic years help me develop the fundamental and essential academic competence.

Last but not least, my sincere appreciation will go to all the members in department of clinical and analytical biochemistry for their sincere friendship, kind assistance and continual encouragements.

## References

- 1) Kjellen, L., Lindahl, U., Proteoglycans: structures and interactions, *Annu. Rev. Biochem.*, **60**, 443-475 (1991).
- 2) Hook, M., Kjellen, L., Johansson, S., Robinson, J., Cell-surface glycosaminoglycans, *Annu. Rev. Biochem.*, **53**, 847-869 (1984).
- 3) Wolfmann M.L., Juliano, B.O., Chondroitin sulfate modifications. I. Carboxyl-reduced chondroitin and chondrosine, *J. Am. Chem. Soc.*, **82**, 1673-1677 (1960).
- 4) Wolfmann M.L., Juliano, B.O., Chondroitin sulfate modifications. II. Sulfated and *N*-deacetylated preparations, *J. Am. Chem. Soc.*, **82**, 2588-2592 (1960).
- 5) Cervigni, M., Natale, F., Nasta, L., Mako, A., Intravesical hyaluronic acid and chondroitin sulphate for bladder pain syndrome/interstitial cystitis: long-term treatment results, *Int Urogynecol J*, **23**, 1187-1192 (2012).
- 6) Gabay, C., Medinger-Sadowski, C., Gascon, D., Kolo, F., Finckh, A., Symptomatic effects of chondroitin 4 and chondroitin 6 sulfate on hand osteoarthritis: a randomized, double-blind, placebo-controlled clinical trial at a single center. *Arthritis Rheum.*, **63**, 3383–3391 (2011).
- 7) Reginster, J.Y., In people with hand osteoarthritis, chondroitin sulphate therapy for 6 months improves pain and function compared with placebo. *Evid Based Med.*, **17**, 152–153 (2012).
- 8) Dechant, J.E., Baxter, G.M., Frisbie, D.D., Trotter, G.W., McIlwraith, C.W., Effects of glucosamine hydrochloride and chondroitin sulphate, alone and in combination, on normal and interleukin-1 conditioned equine articular cartilage explant metabolism. *Equine Vet. J.*, **37**, 227-231 (2005).
- 9) Simanek, V., Kren, V., Ulrichova, J., Gallo, J., The efficacy of glucosamine and chondroitin sulfate in the treatment of osteoarthritis: Are these saccharides drugs or nutraceuticals? *Biomed Pap Med Fac Univ Palacky Olomouc Czech Repub.*, **149**, 51-56 (2005).
- 10) Ishimaru, J.I., Ogi, N., Mizuno, S., Goss, A.N., Quantitation of chondroitin-sulfates, disaccharides and hyaluronan in normal, early and advanced osteoarthritic sheep temporomandibular joints, *Osteoarthritis Cartilage.*, **9**, 365-370 (2001).

- 11) Jackson, C.G., Plaas, A.H., Sandy, J.D., Hua, C., Kim-Rolands, S., Barnhill, J.G., Harris, C.L., Clegg, D.O., The human pharmacokinetics of oral ingestion of glucosamine and chondroitin sulfate taken separately or in combination, *Osteoarthritis Cartilage.*, **18**, 297–302 (2010).
- 12) Clegg, D.O., Reda, D.J., Harris, C.L., Klein, M.A., O'Dell, J.R., Hooper, M.M., Bradley, J.D., Bingham, C.O., 3rd, Weisman, M.H., Jackson, C.G., Lane, N.E., Cush, J.J., Moreland, L.W., Schumacher, H.R., Jr, Oddis, C.V., Wolfe, F., Molitor, J.A., Yocum, D.E., Schnitzer, T.J., Furst, D.E., Sawitzke, A.D., Shi, H., Brandt, K.D., Moskowitz, R.W., Williams, H.J., Glucosamine, chondroitin sulfate, and the two in combination for painful knee osteoarthritis, *N. Engl. J. Med.*, **354**, 795–808 (2006).
- 13) Baici, A., Hörler, D., Moser, B., Hofer, H.O., Fehr, K., Wagenhäuser, F.J., Analysis of glycosaminoglycans in human serum after oral administration of chondroitin sulfate, *Rheumatol. Int.*, **12**, 81–88 (1992).
- 14) Kubo, M., Ando, K., Mimura, T., Matsusue, Y., Mori, K., Chondroitin sulfate for the treatment of hip and knee osteoarthritis: current status and future trends, *Life Sci.*, **85**, 477–483 (2009).
- 15) Harenberg, J., Pharmacology of low molecular weight heparins, *Semin. Thromb. Hemost.*, **16**: 12–18 (1990).
- 16) Johnson, E.A., Mulloy, B., The molecular weight range of commercial heparin preparations, *Carbohydr. Res.*, **51**: 119–127 (1976).
- 17) Andreson, L.O., Barrowcliffe, T.W., Holmer, E., Johnson, E.A., Sims, G.E., Anticoagulant properties of heparin fractionated by affinity chromatography on matrix-bound antithrombin III and by gel filtration. *Thromb. Res.* **9**: 575–583 (1976).
- 18) Linhardt, R. J., 2003 Claude, S. Hudson award address in carbohydrate chemistry. Heparin: structure and activity. *J Med Chem.*, **46**, 2551–2564 (2003).
- 19) Munoz, E. M., Linhardt, R. J., Heparin-binding domains in vascular biology. *Arterioscler Thromb Vasc Biol.*, **24**, 1549–1557 (2004).
- 20) Capila, I., Linhardt, R. J., Heparin–protein interactions, *Angew Chem Int Ed Engl.*, **41**, 391–412 (2002).
- 21) Igarashi, K., Kashiwagi, K., Modulation of protein synthesis by polyamines, *IUBMB Life*, **67**, 160–169 (2015).
- 22) Nishimura, K., Shiina, R., Kashiwagi, K., Igarashi, K., Decrease in polyamines with aging and their ingestion from food and drink, *J. Biochem.*, **139**, 81–90 (2006).



- 23) Higashi, K., Terui, Y., Suganami, A., Tamura, Y., Nishimura, K., Kashiwagi, K., Igarashi, K., Selective structural change by spermidine in the bulged-out region of double-stranded RNA and its effect on RNA function, *J. Biol. Chem.*, **283**, 32989–32994 (2008).
- 24) Basu, H.S., Marton, L.J., The interaction of spermine and pentamines with DNA, *Biochem. J.*, **244**, 243–246 (1987).
- 25) Vijayanathan, V., Thomas, T., Shirahata, A., Thomas, T.J., DNA condensation by polyamines: a laser light scattering study of structural effects, *Biochemistry*, **40**, 13644–13651 (2001).
- 26) Minyat, E.E., Ivanov, V.I., Kritzyn, A.M., Minchenkova, L.E., Schyolkina, A.K., Spermine and spermidine-induced B to A transition of DNA in solution, *J. Mol. Biol.*, **128**, 397–409 (1978).
- 27) Hou, M.H., Lin, S.B., Yuann, J.M., Lin, W.C., Wang, A.H., Kan, L.S., Effects of polyamines on the thermal stability and formation kinetics of DNA duplexes with abnormal structure, *Nucleic Acids Res.*, **29**, 5121–5128 (2001).
- 28) Terui, Y., Ohnuma, M., Hiraga, K., Kawashima, E., Oshima, T., Stabilization of nucleic acids by unusual polyamines produced by an extreme thermophile, *Thermus thermophilus*, *Biochem. J.*, **388**, 427–433 (2005).
- 29) Ruan, G.X., Zhang, T.Y., Li, L.M., Zhang, X.G., Shen, Y.Q., Tabata, Y., Gao, J.Q., Hepatic-targeted gene delivery using cationic mannan vehicle, *Mol. Pharm.*, **11**, 3322–3329 (2014).
- 30) Vijayanathan, V., Agostinelli, E., Thomas, T., Thomas, T.J., Innovative approaches to the use of polyamines for DNA nanoparticle preparation for gene therapy, *Amino Acids*, **46**, 499–509 (2014).
- 31) Kim, H.J., Takemoto, H., Yi, Y., Zheng, M., Maeda, Y., Chaya, H., Hayashi, K., Mi, P., Pittella, F., Christie, R.J., Toh, K., Matsumoto, Y., Nishiyama, N., Miyata, K., Kataoka, K., Precise engineering of siRNA delivery vehicles to tumors using polyion complexes and gold nanoparticles, *ACS Nano*, **8**, 8979–8991 (2014).
- 32) Fernandes, J.C., Qiu, X., Winnik, F.M., Benderdour, M., Zhang, X., Dai, K., Shi, Q., Linear polyethylenimine produced by partial acid hydrolysis of poly(2-ethyl-2-oxazoline) for DNA and siRNA delivery in vitro, *Int J Nanomedicine*, **8**, 4091–4102 (2013).
- 33) Fukumoto, Y., Obata, Y., Ishibashi, K., Tamura, N., Kikuchi, I., Aoyama, K., Hattori, Y., Tsuda, K., Nakayama, Y., Yamaguchi, N., Cost-effective gene transfection by DNA compaction at pH 4.0 using acidified, long shelf-life polyethylenimine, *Cytotechnology*, **62**, 73–82 (2010).

- 34) Tamura, A., Oishi, M., Nagasaki, Y., Enhanced cytoplasmic delivery of siRNA using a stabilized polyion complex based on PEGylated nanogels with a cross-linked polyamine structure, *Biomacromolecules*, **10**, 1818–1827 (2009).
- 35) Toyotama, A., Yamanaka, J., Yonese, M., Photocontrol of polyion complex formation between polylysine and chondroitin sulfate in the presence of pararosaniline leucohydroxide, *Colloid Polym Sci*, **280**, 539–546 (2002).
- 36) Rodén, L., “Structure and metabolism of connective tissue proteoglycans” Chap.7, ed. by Lennarz W.J., *The Biochemistry of Glycoproteins and Proteoglycans*. Plenum Press, New York, 1980, pp. 267–371.
- 37) Higashi, K., Okamoto, Y., Mano, T., Wada, T., Toida, T., A simple HPLC method for identification of the origin of chondroitin sulfate in health foods, *JJFCS*, **21**, 187–194 (2014).
- 38) Volpi, N., Quality of different chondroitin sulfate preparations in relation to their therapeutic activity, *J. Pharm. Pharmacol.*, **61**, 1271–1280 (2009).
- 39) Lippiello, L., Woodward, J., Karpman, R., Hammad, T.A., In vivo chondroprotection and metabolic synergy of glucosamine and chondroitin sulfate, *Clin. Orthop. Relat. Res.*, **381**, 229–240 (2000).
- 40) Nasonov, E.L., Alekseeva, L.I., Chondroitin sulfate (structum) in the treatment of osteoarthritis: pathogenetic rationale and clinical efficacy, *Ter. Arkh.*, **73**, 87–89 (2001).
- 41) Saito, T., Takeuchi, R., Mitsuhashi, S., Uesugi, M., Yoshida, T., Koshino, T., Use of joint fluid analysis for determining cartilage damage in osteonecrosis of the knee, *Arthritis Rheum.*, **46**, 1813–1819 (2002).
- 42) Wang, J.Y., Roehrl, M.H., Glycosaminoglycans are a potential cause of rheumatoid arthritis, *Proc. Natl. Acad. Sci. U.S.A.*, **99**, 14362–14367 (2002).
- 43) Xiao, Y.L., Li, P.L., Cheng, Y.N., Zhang, X.K., Sheng, J.Z., Wang, D.C., Li, J., Zhang, Q., Zhong, C.Q., Cao, R., Wang, F.S., Enhancing the intestinal absorption of low molecular weight chondroitin sulfate by conjugation with  $\alpha$ -linolenic acid and the transport mechanism of the conjugates, *Int J Pharm*, **465**, 143–158 (2014).
- 44) Sahay, G., Alakhova, D.Y., Kabanov, A.V., Endocytosis of nanomedicines, *J Control Release*, **145**, 182–195 (2010).
- 45) Igarashi, N., Takeguchi, A., Sakai, S., Akiyama, H., Higashi, K., Toida, T., Effect of molecular sizes of chondroitin sulfate on interaction with L-selectin, *International Journal of Carbohydrate Chemistry* 2013, 9 pages (2013).
- 46) Higashi, K., Hosoyama, S., Ohno, A., Masuko, S., Yang, B., Sterner, E., Wang,

- Z., Linhardt, R.J., Toida, T., Photochemical preparation of a novel low molecular weight heparin, *Carbohydr Polym*, **67**, 1737–1743 (2012).
- 47) Higashi, K., Ly, M., Wang, Z., Masuko, S., Bhaskar, U., Sterner, E., Zhang, F., Toida, T., Dordick, J.S., Linhardt, R.J., Controlled photochemical depolymerization of K5 heparosan, a bioengineered heparin precursor, *Carbohydr Polym*, **86**, 1365–1370 (2011).
  - 48) Oshima, T., Moriya, T., Terui, Y., Identification, chemical synthesis, and biological functions of unusual polyamines produced by extreme thermophiles, *Methods Mol. Biol.*, **720**, 81–111 (2011).
  - 49) Alam, F., Al-Hilal, T.A., Chung, S.W., Seo, D., Mahmud, F., Kim, H.S., Kim, S.Y., Byun, Y., Oral delivery of a potent anti-angiogenic heparin conjugate by chemical conjugation and physical complexation using deoxycholic acid, *Biomaterials*, **35**, 6543–6552 (2014).
  - 50) Khatun, Z., Nurunnabi, M., Cho, K.J., Byun, Y., Bae, Y.H., Lee, Y.K., Oral absorption mechanism and anti-angiogenesis effect of taurocholic acid-linked heparin-docetaxel conjugates, *J Control Release*, **177**, 64–73 (2014).
  - 51) Al-Hilal, T.A., Alam, F., Park, J.W., Kim, K., Kwon, I.C., Ryu, G.H., Byun, Y., Prevention effect of orally active heparin conjugate on cancer-associated thrombosis, *J Control Release*, **195**, 155–161 (2014).
  - 52) Al-Hilal, T.A., Park, J., Alam, F., Chung, S.W., Park, J.W., Kim, K., Kwon, I.C., Kim, I.S., Kim, S.Y., Byun, Y., Oligomeric bile acid-mediated oral delivery of low molecular weight heparin, *J Control Release*, **175**, 17–24 (2014).
  - 53) Sharmin, S., Sakata, K., Kashiwagi, K., Ueda, S., Iwasaki, S., Shirahata, A., Igarashi, K., Polyamine cytotoxicity in the presence of bovine serum amine oxidase, *Biochem. Biophys. Res. Commun.*, **282**, 228–235 (2001).
  - 54) Yan, Y., Kolachala, V., Dalmasso, G., Nguyen, H., Laroui, H., Sitaraman, S.V., Merlin, D., Temporal and spatial analysis of clinical and molecular parameters in dextran sodium sulfate induced colitis, *PLoS ONE*, **4**, e6073 (2009).
  - 55) Linhardt, R.J., Gunay, N.S., Production and chemical processing of low molecular weight heparins, *Semin. Thromb. Hemost.*, **25**, 5–16 (1999).
  - 56) Hirsh, J., Raschke, R., Heparin and low-molecular-weight heparin, *Chest.*, **126**, 188S–203S (2004).
  - 57) Green, D., Hirsh, J., Heit, J., Prins, M., Davidson, B., Lensing, A.W., Low molecular weight heparin: a critical analysis of clinical trials, *Pharmacol. Rev.*, **46**, 89–109 (1994).
  - 58) Breddin, H.K., Fareed, J., Bender, N., Low molecular weight heparins,

- Haemostasis*, **18**, 1–87 (1988).
- 59) Sheng, J., Han, L., Qin, J., Ru, G., Li, R., Wu, L., Cui, D., Yang, P., He, Y., Wang, J., *N*-trimethyl chitosan chloride-coated PLGA nanoparticles overcoming multiple barriers to oral insulin absorption, *ACS Appl Mater Interfaces*, **7**, 15430–15441 (2015).
- 60) Jain, S., Patil, S.R., Swarnakar, N.K., Agrawal, A.K., Oral delivery of doxorubicin using novel polyelectrolyte-stabilized liposomes (layersomes), *Mol. Pharm.*, **9**, 2626–2635 (2012).

## **List of publication**

1. Poly-ion Complex of Chondroitin Sulfate and Spermine and its Effect on Oral Chondroitin Sulfate Bioavailability. Dan Ge, Kyohei Higashi, Daichi Ito, Yusuke Terui, Kenichi Nagano, Ryota Ishikawa, Kenjiro Higashi, Kunikazu Moribe, Robert J. Linhardt, and Toshihiko Toida  
*Chem. Pharm. Bull.* in press (2016), accepted on Feb. 3<sup>rd</sup>, 2016

## **Dissertation committee**

This dissertation was evaluated by the following committee authorized by the Graduate School of Pharmaceutical Science, Chiba University.

Professor Kousei Ito, Ph.D.      Chairman

(Graduate School of Pharmaceutical Science, Chiba University)

Professor Hiroto Kawashima, Ph.D.

(Graduate School of Pharmaceutical Science, Chiba University)

Professor Kunikazu Moribe, Ph.D.

(Graduate School of Pharmaceutical Science, Chiba University)